WELDING RESEARCH

SUPPLEMENT TO THE *WELDING JOURNAL*, APRIL 1993
Sponsored by the American Welding Society and the Welding Research Council

An Evaluation of Heat-Affected Zone Liquation Cracking Susceptibility, Part I: Development of a Method for Quantification

A material-specific quantification of liquation cracking susceptibility was developed using the hot-ductility, spot- and longitudinal-Varestraint tests

BY W. LIN, J. C. LIPPOLD AND W. A. BAESLACK III

ABSTRACT. A new methodology has been developed for quantifying heat-affected zone (HAZ) liquation cracking susceptibility. This methodology characterizes a thermal crack-susceptible region (CSR) in the HAZ. The thermal CSR was theoretically derived based on the ductility of a material during welding as obtained from the Gleeble hot-ductility test and the criteria assumed in the development of liquation cracking theories. This CSR was experimentally verified using longitudinal- and spot-Varestraint tests performed on A-286 and Type 310 stainless steels. The thermal CSR is material-specific and represents a true quantification of liquation cracking susceptibility. The development of this methodology has 1) elucidated the physical relationship among weldability test results, liquation cracking theories and material properties; 2) provided a more precise interpretation of hot-ductility, spot- and longitudinal-Varestraint tests; 3) defined a method for determining a material-specific measure of HAZ liquation cracking susceptibility; 4) eliminated the inconsistency among certain weldability test results; 5) added important insight regarding the mechanics of HAZ liquation cracking, and 6) confirmed the criterion assumed in the development of liquation cracking theories, which states that cracking results from the localized loss of grain boundary ductility due to liquation. This paper addresses the theoretical background and experimental procedure involved in the development of the methodology. A subsequent paper will describe the metallurgical basis for HAZ liquation cracking as it relates to this methodology.

W. LIN and J. C. LIPPOLD are with Edison Welding Institute, Columbus, Ohio. W. A. BAESLACK III is with The Ohio State University, Columbus, Ohio.

Presented at the 73rd Annual AWS Meeting, held March 22–27, 1992, in Chicago, Ill.

KEY WORDS

Brittle Temperature Range
Crack-Susceptible Region
Heat-Affected Zone
HAZ Liquation Cracking
Hot-Ductility Test
Liquation Cracking
Stainless Steels
Varestraint Test
Weldability
Weldability Test Technique

Introduction

HAZ liquation cracking is a type of high-temperature weld cracking that occurs in the HAZ adjacent to the fusion boundary (Ref.1). This type of cracking is often encountered during the welding of a variety of engineering alloys. It is particularly prevalent in nickel- and aluminum-based alloys, and in fully austenitic stainless steels. The metallurgical basis for cracking involves the presence and persistence of liquid films at grain boundaries and the inability of these films to accommodate the thermally and/or mechanically induced strain experienced during weld cooling. Although the precise mechanisms for liquation cracking are not fully understood, it is recognized that the simultaneous presence of a crack-susceptible microstructure and a critical level of restraint is necessary to promote cracking. Since the control of weld restraint is often difficult, reduction in liquation cracking susceptibility is normally achieved by adjusting the composition and microstructure.

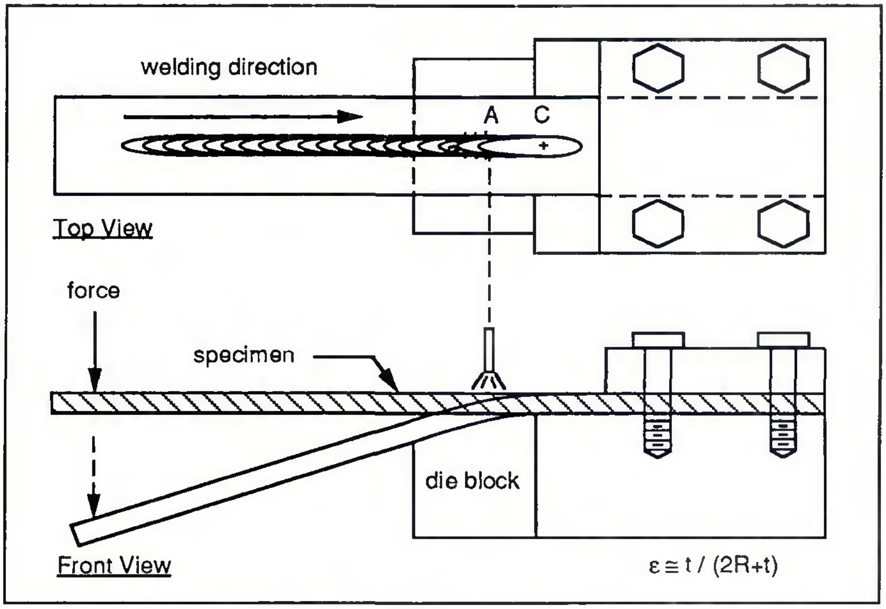

Fig. 1 — Schematic illustration of the longitudinal-Varestraint test.

Since the 1950s, the effects of composition and microstructure on liquation cracking susceptibility have been studied extensively using weldability testing techniques. To date, over 150 separate and distinct techniques have been developed to quantify weld solidification and HAZ liquation cracking susceptibility (Ref. 2). These tests vary widely in their approach and utility, but can generally be classified as representative (self-restraint) or simulative (augmented restraint) test techniques (Refs. 3, 4).

Representative test techniques, such as the circular patch test, seek to reproduce the actual welding condition as closely as possible in an effort to accurately "represent" the situation of interest. These tests depend on self-restraint induced by the specimen design and/or fixturing. In most cases, these test techniques only provide a simple "crack or no crack" solution for a specific material/process/restraint combination. They are ineffective in quantifying weldability among different materials because of the difficulties in isolating the material factor from the test results.

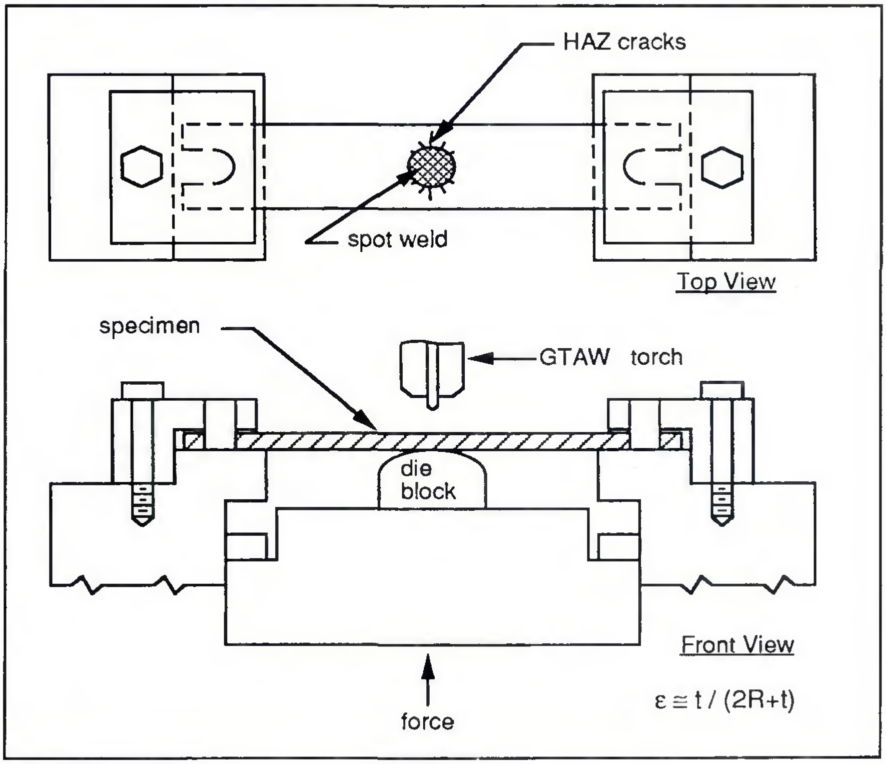

Fig. 2 — Schematic illustration of the spot-Varestraint test.

Simulative test techniques, such as the Varestraint test, attempt to simulate some aspect of the thermomechanical response of the material to the welding process. These tests normally involve the application of an external augmented stress or strain whose magnitude can be easily quantified. The thermally induced restraint of the specimen and/or fixturing is usually negligible compared with the relatively large amount of externally applied stress or strain. This approach allows the metallurgical and compositional factors associated with cracking to be isolated from the mechanical factors, and permits their effects to be studied and quantified. As a result, simulative tests have been successful in providing a comprehensive order ranking of families of alloys or heats of a given alloy. However, the test conditions, especially the combination of thermal and mechanical history, are inherently different from actual welding conditions. According to the technological strength theory (Refs. 5, 6), the ductility of a material varies in a weld thermal cycle. The temperature at which a critical level of strain is applied on a material during weldability testing may be different from that under actual welding conditions. This difference may result in disparate cracking behavior in the simulative test relative to actual practice.

The approach used to discern the effects of test conditions on the cracking behavior relies on developing a physical link between weldability test results and the metallurgical response of the material during testing. The absence of such a link in essentially all weldability test techniques, however, has created difficulties in standardizing the test procedures and resulted in poor reproducibility and correlation. Discrepancies between test results and field experience are not uncommon.

Despite these drawbacks, weldability testing is generally perceived as an efficient and economical method for predicting susceptibility to liquation-related cracking during welding. Among the weldability testing techniques, the longitudinal-Varestraint (mini-Varestraint), spot-Varestraint and hot-ductility tests are three of a few methods that can be utilized in quantifying the HAZ liquation cracking susceptibility or developing a fundamental understanding of the cracking phenomena. Despite their widespread use, there has been little effort to correlate the data generated by these tests or to rigorously apply these data to real-world situations.

Longitudinal-Varestraint test

The original Varestraint test was developed by Savage, *et al.* (Refs. 7, 8), at Rensselaer Polytechnic Institute in the mid-60s, and soon became one of the most widely utilized weldability testing techniques for quantifying the susceptibility of a material to weld solidification cracking. Since that time, three modified versions have been developed based on the original Varestraint concept, namely, the mini-Varestraint (or subscale Varestraint) test, the spot-Varestraint test (originally called the Tigamajig test) (Ref. 9), and the Transvarestraint test (Ref. 10). The mini-Varestraint test uses a smaller test sample, nominally 163 X 25 X 6.4 mm (6.5 X 1 X 0.25 in.) as compared with the original Varestraint test, nominally 300 X 50 X 12.7 mm (12 X 2 X 0.5 in.). In order to avoid confusion with the spot-Varestraint and Transvarestraint tests, the mini-Varestraint (or subscale Varestraint) test is called the longitudinal-Varestraint test in this report. Although this test is utilized primarily for characterizing weld solidification cracking, it has also been used to determine HAZ liquation cracking susceptibility (Refs. 11–15).

A schematic of the longitudinal-Varestraint test is shown in Fig. 1. A specimen is supported as a cantilever beam and a gas tungsten arc weld (GTAW) is produced along the center section of the specimen. When the arc approaches the center of a radiused die block (marked A in Fig. 1), a pneumatically operated ram is triggered forcing the specimen to conform to the surface of the die block. Meanwhile, the arc travels onward and is subsequently interrupted in the run-off area C. Two auxiliary bending bars are added in order to ensure that the specimen conforms to the contour of the die block. The applied augmented strain (ε) of the top surface of the specimen can be varied by adjusting the radius of the die block (R) following the equation, $\varepsilon = t / (2R + t)$, where t is the specimen thickness. In this manner, both weld solidification cracks and HAZ liquation cracks can be produced. The HAZ liquation cracks are normally located adjacent and perpendicular to the fusion boundary.

Cracking susceptibility is assessed by measuring the length of each crack on the as-tested specimen surface. The threshold strain (Appendix B) to cause cracking and the degree of cracking at a specific strain level have been generally utilized as cracking indexes (Refs. 11–15). The degree of cracking can be quantified by the maximum crack length (MCL), the total crack length (TCL) or the cracked HAZ length (CHL) (see Appendix B for definition of terms).

Table 1 — Criteria for Interpreting Hot-Ductility Test Results for HAZ Cracking Assessments

Criterion	Authors, (Refs.)	Year
Classification of hot ductility curves	Nippes, *et al.* (25, 26)	1955
Incorporation of the extent of ductility and strength recovery	Williams (27), Kreischer (28), Weiss, *et al.* (29)	1963
Nil-ductility temperature range between the NST and DRT	Williams (27), Dahl, *et al.* (30, 31), Donati, *et al.* (11)	1963
The extent of the nil-ductility region and the amount and rate of ductility recovery on-cooling	Duvall, *et al.* (32–33)	1966
The zero ductility range and mid-temperature ductility dip range	Yeniscavich (34, 35)	1966
The temperature range between the NDT and DRT	Arata, *et al.* (36)	1977
The ratio of ductility recovery (RDR), ductility recovery rate (DRR) and nil-ductility temperature range (NDR)	Lundin, *et al.* (14)	1991

Spot-Varestraint Test

The spot-Varestraint test (Ref. 9) has been widely applied for evaluating HAZ liquation cracking susceptibility. A schematic of the test apparatus is shown in Fig. 2. During spot-Varestraint testing, a GTA spot weld is produced in the center section of a small specimen, nominally 140 X 25 X 6.4 mm (5.5 X 1 X 0.25 in.). After a predetermined weld time, the arc is extinguished and the specimen is forced to conform to the surface of a radiused die block. In this manner, HAZ liquation cracks can be generated on the surface of the specimen adjacent to the GTA spot weld. The applied augmented strain (ε) of the top surface of the specimen is approximated in the same manner as for the longitudinal-Varestraint test.

Cracking susceptibility is determined by measuring the length of each crack on the as-tested specimen surface. The threshold level of strain to cause cracking or the degree of cracking (quantified by MCL or TCL) over a range of strain levels have been generally accepted as cracking indexes since the introduction of this test (Refs. 9, 16–23).

Hot-Ductility Test

The concept in the design of the hot-ductility test is different from the majority of weldability testing techniques. Instead of quantifying the cracking susceptibility by the degree of cracking, it characterizes the ductility of the material at elevated temperatures and relates this ductility data to cracking susceptibility. Basically, small tensile samples are fractured rapidly at some specific temperatures during either the on-heating or on-cooling portion of a duplicated weld thermal cycle in a thermomechanical simulator called a Gleeble™. The transverse reduction-in-area of the fractured sample is subsequently determined providing a measure of ductility.

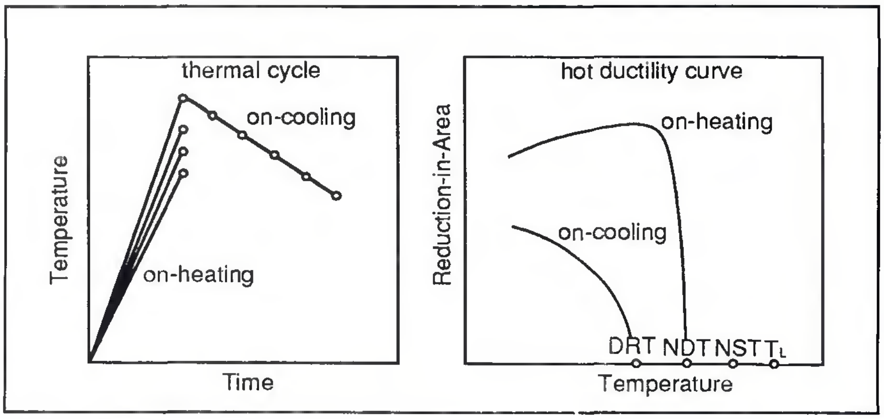

Fig. 3 — Schematic illustration of the hot-ductility test.

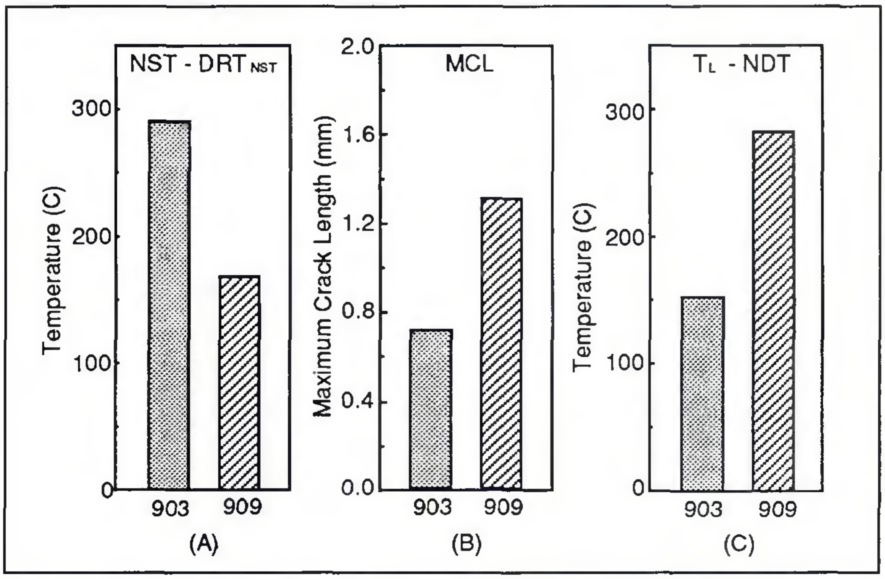

Fig. 4 — Comparison of test results for Incoloy Alloys 903 and 909 from the spot-Varestraint and hot-ductility tests; A — the temperature range between the NST and DRT_{NST} obtained from the hot-ductility test; B — the maximum crack length obtained from the spot-Varestraint test; C — the temperature range between the T_L and NDT obtained from the hot-ductility test (Ref. 37).

Both the on-heating and on-cooling ductility curve in the vicinity of the solidus temperature can be obtained, as shown in Fig. 3, and the nil-ductility temperature (NDT), nil-strength temperature (NST) and ductility recovery temperature (DRT) determined (see Appendix B for definition of terms). In addition to the hot ductility, the hot strength of the material can also be measured.

In the past, experimental methodologies and data interpretation for hot-ductility testing have been the subject of considerable investigation. A review by Lin (Ref. 24) indicated that the methods for interpreting hot-ductility test results for HAZ cracking assessments vary significantly from investigator to investigator. Table 1 lists the several criteria that have been proposed to date. Among these criteria, the extent of the nil-ductility region and the amount and rate of ductility recovery (Refs. 32, 33), and the nil-ductility temperature range between the NST and DRT (Refs. 11, 27, 30, 31) are the most widely accepted.

The hot-ductility and spot-Varestraint tests are normally considered complementary in quantifying HAZ liquation cracking susceptibility and yield qualitatively consistent results. A previous investigation (Ref. 37), however, showed that these two tests were inconsistent in predicting the HAZ liquation cracking susceptibility of Incoloy® Alloys 903 and 909, when "conventional" techniques were used to interpret test results. Figure 4 shows that the MCLs of Incoloy Alloys 903 and 909 as obtained from the spot-Varestraint test (Fig. 4B) were contradictory to the on-cooling nil-ductility temperature range ($NST-DRT_{NST}$) (see appendix for symbols and abbreviations) as obtained from the hot-ductility test — Fig. 4A. However, the MCL correlated very well with the on-heating nil-ductility temperature range (T_L-NDT) — Fig. 4. These results stimulated a research program to fundamentally evaluate the hot-ductility, spot- and longitudinal-Varestraint tests.

Table 2 — Chemical Compositions of A-286 and Type 310 Stainless Steel Investigated in This Study (wt-%)

Element	A-286	Type 310
C	0.054	0.083
Mn	0.19	1.42
P	0.016	0.024
S	0.009	0.004
B	0.006	Not Analyzed
Si	0.25	0.46
Ni	24.22	18.72
Cr	14.58	24.75
Mo	1.32	0.27
Cu	0.10	0.32
Al	0.34	0.062
Ti	2.29	0.014
V	0.22	0.054
Fe	bal.	bal.

Table 3 — Conditions for Hot-Ductility Testing of A-286 and Type 310 Stainless Steels

Heating time: 12.15 s
Holding time at peak temperature: 0.03 s
Cooling rate: 50°C/s (90°F/s)
Holding time at test temperature: 0.03 s
Stroke rate: 5 cm/sec (2 in/s)
Sample freespan: 25 mm (1 in.)
Atmosphere: argon

Objectives

The principal objectives of this study were as follows:

1) Study the physical relationship among weldability test results, cracking theories and material properties.

2) Develop a generic methodology and define a material-specific parameter, based on the hot-ductility, longitudinal- and spot-Varestraint test results, that quantifies HAZ liquation cracking susceptibility.

3) Investigate the correlations among these three techniques.

4) Re-evaluate the current methodologies for interpretation of the three tests in the light of the new methodology which is proposed.

Experimental Design

Materials

A-286 and Type 310 stainless steels were investigated in this study. A-286 is a precipitation-hardened iron-base alloy designed for applications requiring moderately high strength to 700°C (1292°F) and oxidation resistance to about 815°C (1499°F). The excellent room and elevated temperature strengths exhibited by this alloy result from the presence of Ni, Ti and Al, which promote formation of the γ' $Ni_3(Al,Ti)$ strengthening phase. This alloy is often used for jet engine and gas turbine applications due to its highly desirable combination of properties.

Extensive studies in the past have shown this alloy to be susceptible to both weld solidification and HAZ liquation cracking (Refs. 38–41). Vagi, *et al.* (Ref. 40), associated HAZ liquation cracking with the formation of a Fe_2Ti Laves phase. They proposed that grain boundary liquation by the $Fe-Fe_2Ti$ eutectic (1310°C; 2390°F) allows the

Table 4 — Conditions for Longitudinal-Varestraint Testing of A-286 Stainless Steels

Current: 190 A
Voltage: 12 V, DCEN
Travel speed: 2.54 mm/s
Augmented strain: 0.5–7%
Shielding gas: Argon, 30 CFH
Electrode: W-2% ThO_2, 2.4 mm (3/32 in.) diameter., 60-deg included angle
Air Pressure: 0.55 MPa (80 psi)
Strain rate: approximately 13%/s
Weld bead width: 7.5 mm

grains to be separated by thermally induced strain. Blum, *et al.* (Ref. 38), agreed with Vagi, *et al.*, but they also proposed that grain boundary precipitation of a continuous film of TiC and intragranular precipitation of γ' inhibits deformation during cooling, which causes base metal cracks to propagate and relieve the weld stresses. Later works by Brooks (Ref. 41) indicated that the loss of hot ductility above 1150°C (2102°F) was attributed to the presence of boron. He suggested that the constitutional liquation of borides caused grain boundary liquation and resulted in cracking.

Type 310 is a fully austenitic stainless steel developed for applications requiring high corrosion resistance. Due to the fully austenitic nature of the resolidified weld metal, this alloy suffers from weld solidification cracking as well as HAZ liquation cracking (Refs. 20, 42–46). Comparing the HAZ liquation cracking susceptibility of this alloy with other austenitic stainless steels, Kujanpää, *et al.* (Ref. 20), and Morishige, *et al.* (Ref. 42), indicated that Type 310 is more susceptible than Types 316, 347, 321, 304 and 309. A fundamental investigation of the HAZ liquation cracking mechanism of this alloy by Tamura, *et al.* (Ref. 46), suggested that Cr and Ni in the solute-rich zones in the matrix were swept up and assimilated into the migrating grain boundaries during weld thermal cycling. A subsequent eutectic reaction involving Cr and Ni at the grain boundaries caused a depression in the effective solidus.

The chemical compositions of A-286 and Type 310 stainless steels investigated in this study are listed in Table 2. Both materials were in the form of 6.5-mm (0.25-in.) thick plate. A-286 exhibited a recrystallized austenitic structure with a grain size of ASTM No. 9 and contained a bimodal distribution of titanium carbides and/or carbonitrides. Type 310 was fully austenitic with a grain size of ASTM No. 6. Note that the nickel content of Type 310 is slightly lower than the specification limits of 19 to 22%. Both alloys exhibited relatively low levels of impurities, particularly with respect to sulfur and phosphorus contents.

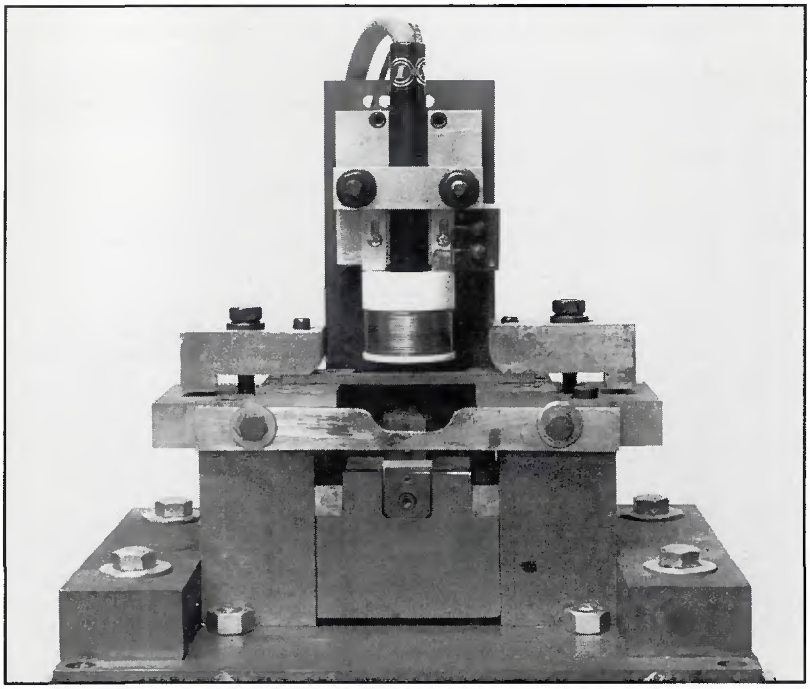

Fig. 5 — Experimental setup for the spot-Varestraint test.

Hot-Ductility Testing

Hot-ductility tests were performed under an argon atmosphere using a Gleeble™ 1000 system. Standard specimens 6.35 mm in diameter and 100 mm long (0.25 X 4 in.) were machined from the plate. A specimen freespan (jaw spacing) of 25 mm (1 in.) was used throughout the investigation. The NST was determined by heating samples at a rate of 111°C/s (200°F/s) under a static load sufficient to overcome the frictional force of the fixture, approximately 10 kg (22 lb). On-heating tests were conducted by heating samples to the peak temperature in 12.15 s and pulling them to failure at a rate of 5 cm/s (2 in./s). The on-heating time to peak temperature was based on the NST test. On-cooling tests were performed after heating to the NST in 12.15 s and cooling to the desired temperature at 50°C/s (90°F/s). This cooling rate was the maximum achievable with the materials and specimen freespan utilized without externally assisted cooling. On-cooling test samples were also pulled to failure at 5 cm/s. This rapid stroke rate was selected to minimize the change in specimen temperature during fracture. Sample ductility, in terms of reduction in area, was subsequently measured using a vernier caliper. The conditions for hot ductility testing are summarized in Table 3.

Longitudinal-Varestraint Testing

Longitudinal-Varestraint tests were performed only on A-286 stainless steel at strains ranging from 0.5 to 7%. Three samples were tested at each strain level on a subscale Varestraint test unit using specimens with dimensions of 163 X 25 X 6.35 mm (6.5 X 1 X 0.25 in). Two auxiliary bending bars were located on each side of the sample to ensure that the specimen fully conformed to the surface of the die block during testing. The conditions for longitudinal-Varestraint testing are listed in Table 4. A rapid strain rate (approximately 13%/s) was selected to minimize the change in specimen temperature in the HAZ during bending. A 7.5-mm (0.3-in.) weld bead width was obtained with these welding parameters.

A binocular microscope with 40X magnification was utilized to identify the locations of each crack tip relative

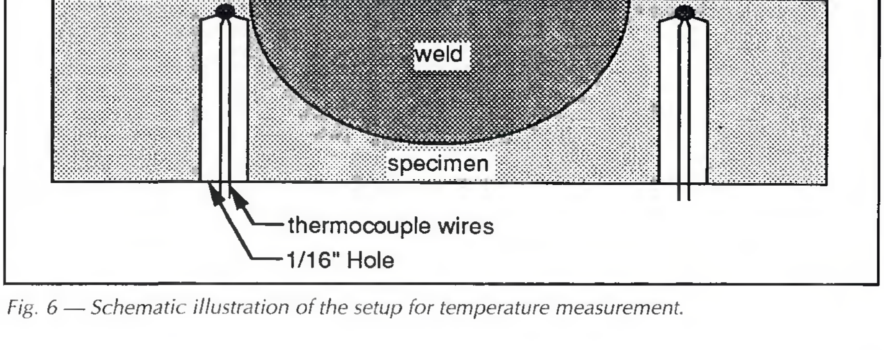

Fig. 6 — Schematic illustration of the setup for temperature measurement.

Table 5 — Conditions for Spot-Varestraint Testing of A-286 and Type 310 Stainless Steels

	A-286	Type 310
Weld time	35 s	35 s
Current	96 A	110 A
Voltage	16 V	12 V
Weld diameter	11.5 mm	12 mm
Shielding gas	Argon, 20 ft^3/h	Argon, 20 ft^3/h
Air pressure	0.55 MPa (80 lb/in.^{2})	0.55 MPa (80 lb/in.^{2})
Strain rate	approximately 13%/s	approximately 13%/s
Augmented strain	0.5–5%	1–7%
Cooling time	0–4.5 s	0–0.45 s
Electrode	W-2%ThO_2, 2.4 mm (3/32 in.) diameter, 60-deg included angle	

Table 6 — Hot-Ductility Test Results of A-286 and Type 310 Stainless Steels

	A-286	Type 310
T_L[a]	1422°C	1386°C
NDT	1200°C	1325°C
NST	1350°C	1350°C
DRT_{NST}	1050°C	1325°C
T_L-NDT	222°C	61°C
NST-DRT_{NST}	300°C	25°C

(a) T_L was determined as the peak temperature experienced at the fusion boundary during spot-Varestraint testing.

to the interception of the instantaneous solid/liquid interface and the fusion boundary. These crack tip locations and the fusion boundary circumscribed a cracked HAZ region. The maximum width of the cracked HAZ was designated as the maximum crack length (MCL), which is the distance between the crack tip of the longest crack and the fusion boundary projecting in a direction perpendicular to the fusion boundary.

Spot-Varestraint Testing

Spot-Varestraint tests were performed on a Tigamajig-type test unit (Ref. 9) using specimens with dimensions of 140 X 25 X 6.35 mm (5.5 X 1 X 0.25 in.). Slots (rather than holes) at both ends of the sample allowed samples to be accurately located and fixtured, and also minimized any axial tensile force during specimen bending. The conditions for spot-Varestraint testing are listed in Table 5. The criterion for determining the welding parameters was to obtain a cooling rate that was comparable with that used during on-cooling hot-ductility testing. For the parameters selected, the average cooling rate from 1350° to 1200°C was about 84°C/s (151°F/s) for A-286 and 112°C/s (202°F/s) for Type 310. The average cooling rate over a wider temperature range, from 1350° to 1000°C, was about 60°C/s (108°F/s) for A-286 and 70°C/s (126°F/s) for Type 310. A rapid strain rate (approximately 13%/s) was also selected to minimize the change in specimen temperature during bending.

The spot-Varestraint tests were conducted in two stages. The first set of tests, called the on-heating spot-Varestraint tests, was aimed at determining the cracking behavior of the material on weld heating. This was achieved by performing the tests with no cooling time (see Appendix B for definition). Thus, the HAZ was on-heating when it was straining. The on-heating spot-Varestraint tests were performed from 0.5 to 7% augmented strain with three samples for each strain level. The second set of spot-Varestraint experiments, called the on-cooling spot-Varestraint tests, was designed to investigate the cracking behavior of the material on weld cooling. This was accomplished by performing the tests above the saturated strain level (see Appendix B for definition) with variable cooling times. The cooling time was varied by adjusting the time period between arc extinction and sample bending. Based on the cracking behaviors of these two alloys, cooling times ranging from 0 to 4.5 s were utilized for A-286 and from 0 to 0.45 s for Type 310.

Because cooling time is a critical parameter in this test, it was precisely calibrated and monitored throughout the test. The actual cooling time is the period between the instant at which the welding current drops to essentially zero and the time at which the die block contacts the specimen. A special setup was devised to precisely monitor the actual cooling time.

It is also important to point out that for Type 310, the weld pool became irregular for weld times longer than about 20 s. In order to produce a uniform circular weld pool, an electromagnetic coil was custom-built and attached to the weld torch as shown in Fig. 5. The size of the coil is 25 mm in height with 35-mm ID and 50-mm OD (1 in. H X 1.375 in. ID X 2 in. OD). There were 280 turns of 19-gauge wire in this coil. By energizing this coil with 4.0 A of alternating current, the weld pool could be forced to rotate, resulting in a symmetrical, circular pool shape.

Quantitative cracking data were obtained from as-tested samples by measuring the length of the longest crack between the fusion boundary and crack tip projecting in a direction perpendicular to the fusion boundary using a binocular microscope under 40X magnification. Thus, the maximum crack length (MCL) reported here represents the distance between the isotherms at the crack tip and the fusion boundary, rather than the actual length of the observed crack.

Thermal Cycle Measurement

The thermal cycles experienced during both the spot- and longitudinal-Varestraint testing were measured using fine wire S-type (Pt - Pt 10%Rh, 0.2 mm in diameter) and K-type (Chromel and Alumel, 0.25 mm in diameter) thermocouples. K-type thermocouples were utilized only to measure the thermal cycles with a peak temperature below 1350°C. These thermocouples were percussion welded at the bottom of 1.6 mm (1/16 in.) holes, which were drilled from the bottom of specimens to within about 0.3 mm from the surface on which the weld was placed, as shown in Fig. 6. The temperature was recorded using a Labtech Notebook software package (Ref. 47) at

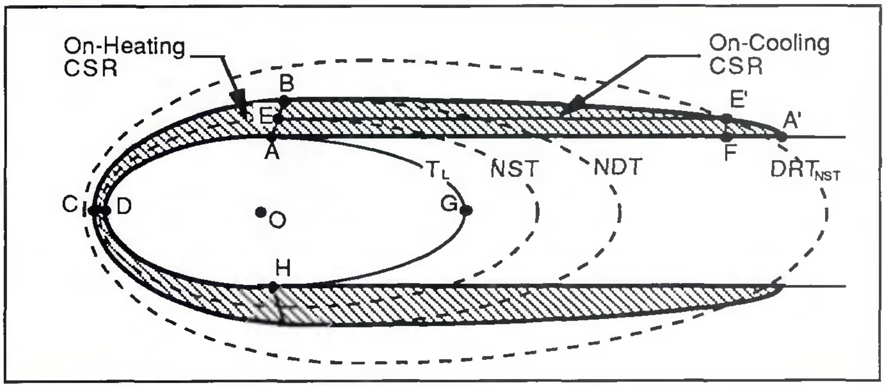

Fig. 7 — Theoretical hypothesis of the thermal crack-susceptible region.

a sampling rate of 20 Hz on an IBM 386 compatible personal computer. Under these conditions, the thermal cycles at different locations from the fusion boundary into the HAZ were obtained. The peak temperatures and cooling rates were determined and temperature gradients approximated.

Metallurgical Characterization

Representative longitudinal- and spot-Varestraint test specimens were metallographically prepared by grinding about 0.2 mm (0.008 in.) of material from the top surface and then polishing through 0.05-micron alumina. Hot-ductility specimens were ground to the center section of the sample and then polished through 0.05-micron alumina. Both A-286 and Type 310 stainless steels were etched with a mixed acid solution comprised of equal parts of concentrated nitric, hydrochloric and acetic acids. Microstructures were characterized using an optical microscope at magnifications up to 1000X.

Development of the Crack-Susceptible Region

Theoretical Hypothesis of the Thermal Crack-Susceptible Region

Metallurgically, HAZ liquation cracking is associated with the occurrence of grain boundary liquation. In the past, most efforts in studying HAZ liquation cracking mechanisms have been directed toward characterizing the evolution and distribution of liquid in the HAZ. However, the mere presence of liquid films at grain boundaries is not sufficient to induce a liquation crack. In order to cause cracking, it is essential that the crack-susceptible microstructure be subjected to a sufficient tensile strain (or stress). During welding, the tensile strain (or stress) does not generally develop until the weld begins to cool (Ref. 48). As a result, liquation cracking occurs during the solidification of the liquid films. The cooling cycle of the liquid films in the HAZ is similar to the final stages of weld solidification, although the origin of the liquid films and the microstructural boundaries may be different from those present in the weld metal. Consequently, to a first approximation, the criteria that govern weld solidification cracking can be adopted to explain the solidification of liquid and resultant cracking in the HAZ.

Many mechanisms have been proposed to describe weld solidification cracking. Among these, the shrinkage-brittleness theory (Refs. 49–51), the strain theory (Refs. 52–54), the generalized theory (Refs. 55–58), and the technological strength theory (Refs. 5, 6) are the best known. Although these theories differ in their approach to cracking mechanistics, there is general agreement that cracking occurs in a discrete temperature envelope called the brittle temperature range (BTR) (see Appendix B for definition). Metallurgically, the BTR describes a range between the temperature where liquid is confined within the solidification structure to that where the boundary liquid is partially or completely solidified and the material recovers its ductility. Mechanically, the BTR represents the regime over which the ductility of the material is essentially zero and, thus, susceptible to cracking.

The ductility of the material during a weld thermal cycle can be determined

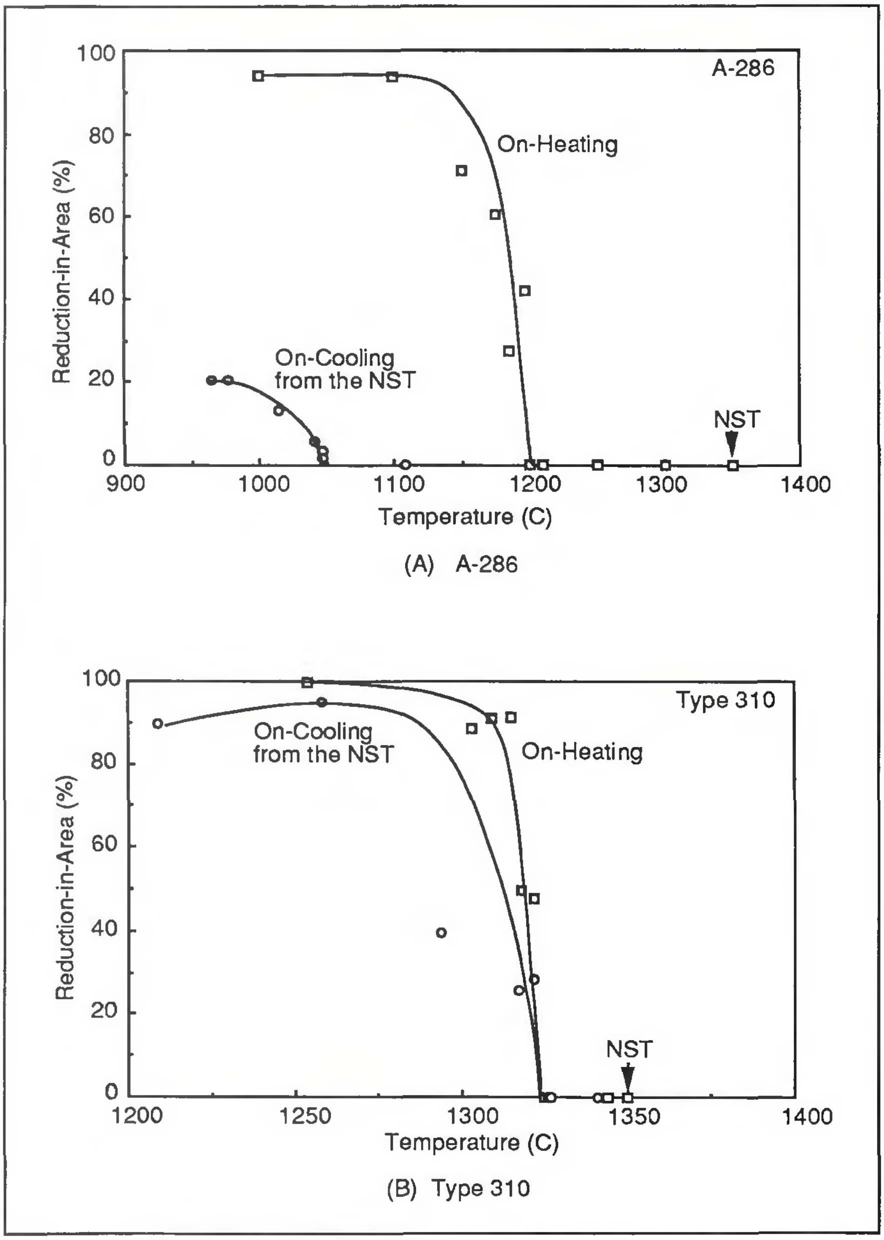

Fig. 8 — Hot-ductility behavior of A-286 and Type 310 stainless steels.

Table 7 — Pertinent Longitudinal-Varestraint Test Results of A-286

	A-286
MCL (at saturated strain = 3%)	0.80 mm
$CHL_{OC,NST}$	11.5 mm
$CHL_{OC,TL}$	14.5 mm
G_T	286°C/mm
CR_T at NST from NST over $CHL_{OC,NST}$, (E-E′ in Fig. 13)	66°C/s
CR_T at T_L from T_L over $CHL_{OC,TL}$, (A-A′ in Fig. 13)	69°C/s

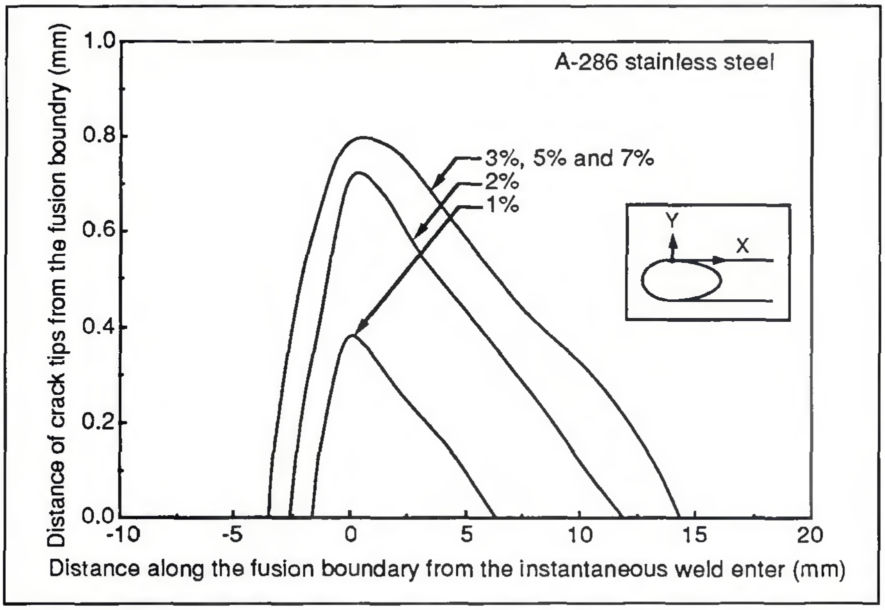

Fig. 9 — The locus of crack tips in the cracked HAZ region for A-286 at different strain levels obtained from the longitudinal-Varestraint test.

using the hot-ductility test. According to this test (Fig. 3), a material loses all ductility when the temperature reaches the NDT on heating and recovers ductility at the DRT on cooling. The hot-ductility test results indicate that there are two temperature ranges within which the material exhibits negligible ductility. These are the on-heating nil-ductility temperature range, which is the temperature regime between the NDT and T_L, and the on-cooling nil-ductility temperature range, which is the temperature range between a peak temperature (T_P) and the corresponding DRT. While the on-heating nil-ductility temperature range is constant, the on-cooling nil-ductility temperature range is a function of the peak temperature. Results from a previous study (Ref. 37) showed that different peak temperatures resulted in a variation in the corresponding DRT. In general, as the peak temperature is increased above the NDT, the DRT decreases, resulting in a net increase in the on-cooling nil-ductility temperature range. From a physical sense, different peak temperatures for the on-cooling test represent different locations in the HAZ. Thus, a peak temperature equal to the liquidus (T_L) would represent a point at the weld fusion boundary, while a peak temperature equal to the NST would represent a point in the HAZ which experiences a thermal cycle with a peak temperature equal to the NST. Farther away from the fusion boundary, the peak temperature decreases rapidly and the corresponding DRT increases.

Based on this discussion, it follows that a nil-ductility region (NDR) (see Appendix B for definition) in the HAZ could be constructed on a temperature field surrounding the weld pool, as illustrated in Fig. 7. Assuming that the weld is progressing from right to left at an instant with the weld center located at point O, the ellipse HDAG represents the instantaneous solid/liquid interface of the weld pool at a temperature equal to the alloy liquidus. The dashed lines represent the isotherms of different temperatures. The fusion boundary is represented by AA′. Point A represents the instantaneous liquidus temperature. Point B represents the point at which the thermal cycle experiences a peak temperature equal to the NDT. CB represents the isotherm of the NDT. Temperatures along the line AB, the transition between on-heating and on-cooling, would then represent various peak temperatures used to determine on-cooling ductility. For each set of the on-cooling hot-ductility tests, a DRT can be determined that is specific to a given peak temperature along AB. This DRT can then be located at the intersection of the DRT isotherm and a line from the point of the peak temperature parallel to the fusion boundary toward the cooling direction, because the DRT and the peak temperature are in the same thermal cycle. For example, Point E and E′ are in the same thermal cycle with a peak temperature equal to the NST. This thermal cycle achieves its peak temperature at point E and falls off along line EE′ reaching the DRT_{NST} isotherm at point E′. Based on the on-cooling hot ductility data, line EE′ represents a regime in which the material exhibits negligible ductility. A similar process can be used to determine the entire DRT curve BA′, as shown in Fig. 7. Thus, the thermal envelope of the NDR is defined by the NDT isotherm, line CB, and the various DRTs, line BA′, for the on-heating and on-cooling behavior, respectively. This NDR represents an area in which the material exhibits negligible ductility. According to the criterion assumed in the development of the liquation cracking mechanisms, which states that cracking results from the localized loss of ductility, this NDR should be equivalent to an area in the HAZ that is susceptible to liquation cracking. By definition, it is the thermal CSR (Appendix B).

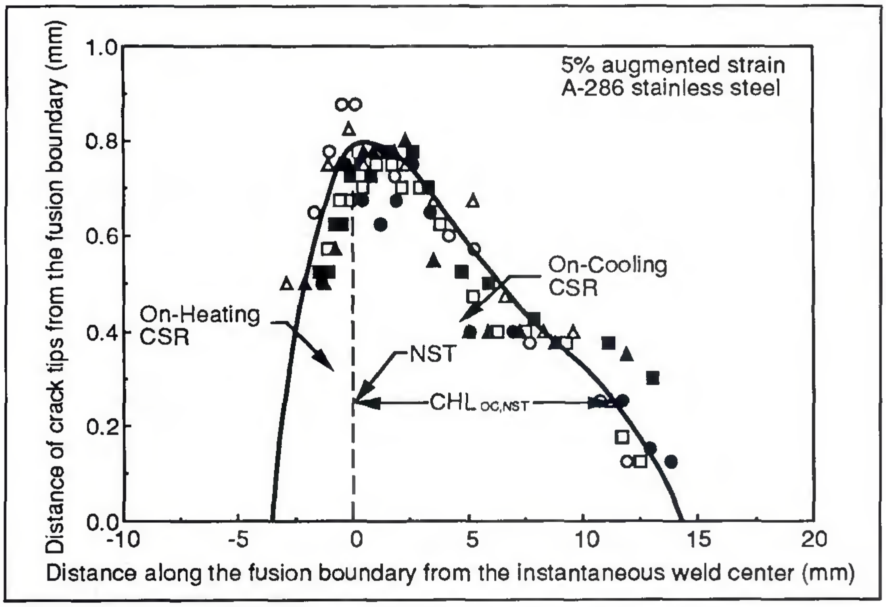

Fig. 10 — The crack-susceptible region (CSR) of A-286 obtained from the longitudinal-Varestraint test. Symbols represent crack tips in both sides of three individual samples, with open and solid from alternate sides of the same sample.

Hot ductility test data are not sufficient, however, to absolutely define the entire thermal CSR in Fig. 7. Since on-cooling hot ductility tests are very difficult to perform using peak temperatures above the NST, the value for the DRT's between point E' and A' in Fig. 7 cannot be obtained using the conventional hot-ductility test.

Hot-Ductility Test Results

In this study, A-286 and Type 310 stainless steels were investigated to verify the proposed hypothesis. The on-heating and on-cooling hot ductility curves for the two alloys are presented in Fig. 8. The NST for both alloys was approximately 1350°C (2462°F). The on-heating ductility of the A-286 decreased rapidly above 1150°C (2102°F) and approached zero at 1200°C (2192°F). On-cooling from the NST, the ductility of this alloy did not recover significantly until it had been cooled to below 1050°C (1922°F). Thus, for A-286, the NDT is 1200°C and the DRT_{NST} is 1050°C. Type 310 stainless steel exhibited similar on-heating ductility behavior with a NDT of 1325°C (2417°F). However, ductility recovery was much more rapid as evidenced by a DRT_{NST} of 1325°C (2417°F). The hot-ductility results (Table 6) indicate that the on-heating nil-ductility temperature ranges (T_L - NDT) for A-286 and Type 310 are 222° and 61°C (400° and 110°F), and the BTR at a point that experiences a peak temperature equal to the NST (NST - DRT_{NST}) are 300° and 25°C (540° and 45°F), respectively.

Experimental Verification of the Thermal Crack-Susceptible Region

The thermal CSR is material-specific and is inherent to the HAZ surrounding weld pools made with any of the conventional fusion welding processes. This region can be revealed by applying a sufficient tensile strain on a material, while a fusion welding process is occurring. This can be effectively achieved using the spot- and longitudinal-Varestraint tests.

Longitudinal-Varestraint Test Results

The longitudinal-Varestraint tests were performed only on A-286, with augmented strain levels ranging from 0.5 to 7%. The locations of each crack tip in the HAZ of the as-tested specimen surface were identified relative to the interception of the instantaneous solid/liquid interface and the fusion boundary. The profile of these crack tips and the fusion boundary circumscribed a cracked HAZ region. It was found that the size of the cracked HAZ region expanded for the strain level ranging from 0.5 to 3% as shown in Fig. 9. Above a saturated strain level of 3%, the size and shape of this cracked HAZ region is essentially constant. This saturated cracked HAZ region was previously defined as a crack-susceptible region (CSR). As shown in Fig. 10, the weld pool progressed from right to left. The CSR expanded on weld heating and shrank upon cooling. The maximum width of the CSR occurs at the transition between the on-heating and on-cooling regions.

The maximum widths of the cracked HAZ region at different strain levels, as defined by the maximum HAZ crack length (MCL), are shown in Fig. 11. The MCL increased as augmented strain increased from 0.5% up to 3%, with a threshold strain of about 0.5%. Above 3% strain the MCL was essentially constant at 0.80 mm (0.03 in.) from the fusion boundary.

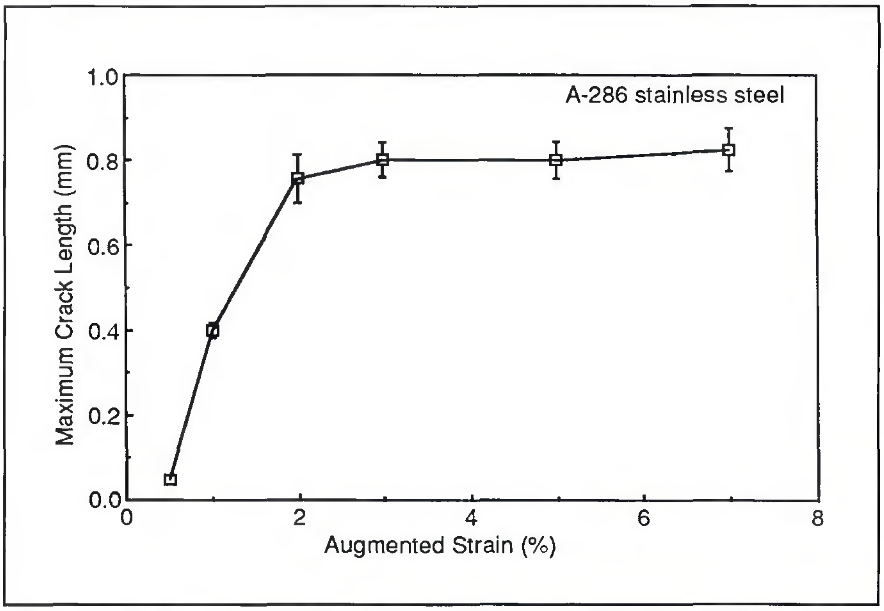

Fig. 11 — The maximum crack length at different augmented strain levels for A-286 obtained from the longitudinal-Varestraint test.

Development of the Thermal CSR Based on the Longitudinal-Varestraint Test Results

The size of the CSR shown in Fig. 10 depends on the material tested and the welding parameters employed during testing. In order to directly compare the CSR among different materials, the welding process variables must be isolated from the material factor. One way to achieve this is to normalize the test results with respect to the thermal conditions the HAZ experienced during test-

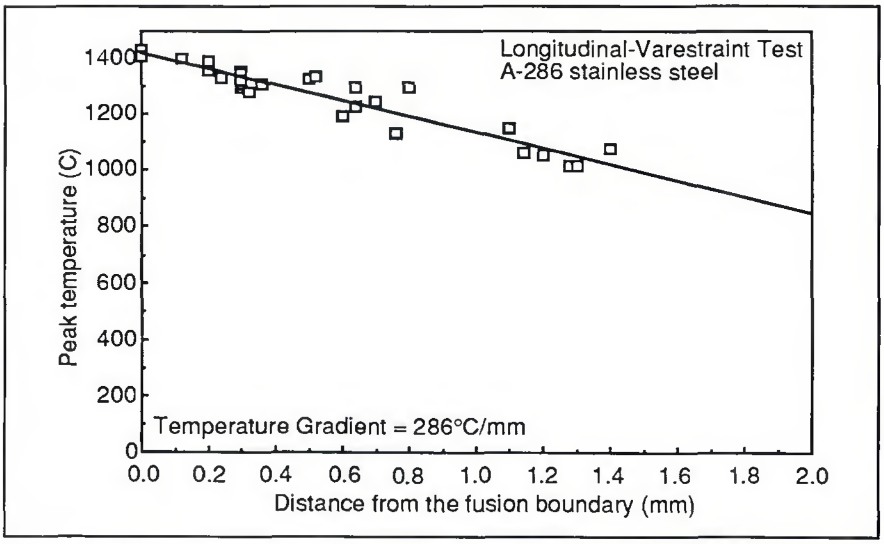

Fig. 12 — Peak temperatures of weld thermal cycles at different locations in the HAZ during longitudinal-Varestraint testing.

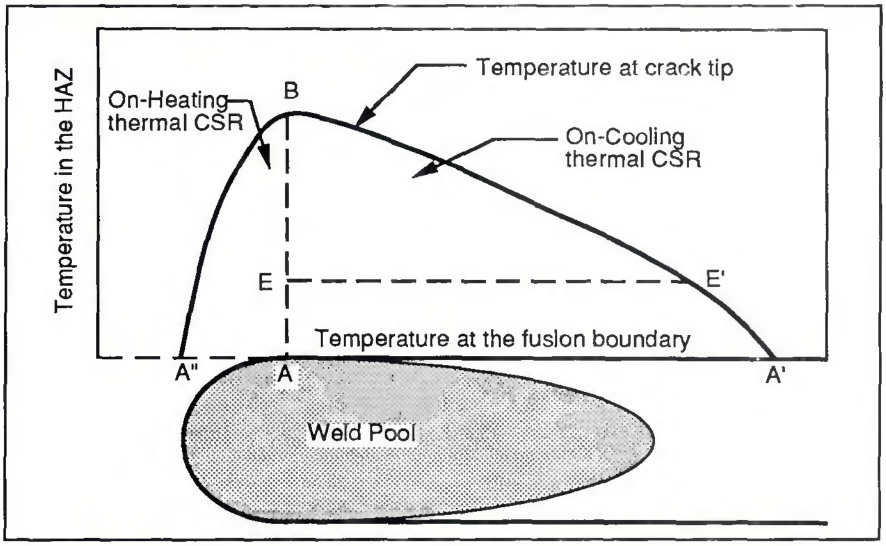

Fig. 13 — Schematic illustration of thermal CSR obtained from the longitudinal-Varestraint test.

ing. This, in fact, provides a material-specific parameter, termed the thermal CSR, which uniquely describes the CSR in terms of temperature.

The thermal conditions of the HAZ during testing of A-286 were obtained using implanted thermocouple wires. The peak temperatures at different locations in the HAZ are shown in Fig. 12. The approximate temperature gradient in the region immediately adjacent to the fusion boundary was 286°C/mm (515°F/0.04 in.).

In conjunction with the thermal cycle data, the spatial CSR (Fig. 10) can be translated into the thermal CSR as illustrated in Fig. 13. The weld is progressing from right to left at an instant when the solid/liquid interface intercepts the fusion boundary at point A. Point A thus represents the instantaneous liquidus temperature (T_L). The temperature at the fusion boundary after the weld pool has passed is represented by AA′. Point B represents the crack tip temperature at the transition between on-heating (left of AB) and on-cooling regions (right of AB). The temperature at Point B (T_B) can be derived by the equation:

$$T_B = T_L - (MCL \times G_T) \qquad (1)$$

where, G_T is the gradient of peak temperatures during longitudinal-Varestraint testing. Temperatures along the line AB would then represent various peak temperatures (T_P) the HAZ experienced during testing. Note that in actual welding fabrication, line AB would incline to the fusion boundary toward cooling direction. With a very narrow peak temperature range from the liquidus, as discussed in this study, this line can be assumed to be perpendicular to the fusion boundary. Line A″BA′ represents the profile of crack tip temperatures. The crack tip temperature (T_{tip}) can be experimentally derived by the following equation using a point along line AB with the same distance from the fusion boundary as a reference.

$$T_{tip} = T_P - (CR_T \times CHL_{OH/OC} / V_T) \qquad (2)$$

where, T_P = the peak temperature of a thermal cycle that the point of interest experienced; $CHL_{OH/OC}$ = the length measured parallel to the fusion boundary between the crack tip and the point which experiences the peak temperature of the same thermal cycle. This length is designated as CHL_{OH} for the crack tip located in the on-heating portion, and CHL_{OC} for the on-cooling portion (Fig. 10); CR_T = the average cooling (or heating) rate over CHL_{OC} (or CHL_{OH}); V_T = welding speed during longitudinal-Varestraint testing.

For example, Point E and E′ are in the same thermal cycle with a peak temperature equal to T_E, as they are equidistant from the fusion boundary. This thermal cycle achieves its peak temperature at point E and falls off along line EE′. Cracking is observed within the area of A″BE′A′A″. Thus, CHL_{OC} at point E is represented by the length EE′. The time required ($t_{EE'}$) for the temperature to fall from point E to point E′ is the distance between these two points (EE′) divided by the welding speed during testing (V_T), $t_{EE'} = EE' / V_T$. The temperature in the thermal cycle reaches point E′ ($T_{E'}$) at a time period $t_{EE'}$ after it has achieved the peak. Or, mathematically, $T_{E'} = T_E - (CR_T \times EE' / V_T)$. CR_T is the average cooling rate from the peak temperature T_E over a time period of $t_{EE'}$. Pertinent thermal CSR data for A-286 obtained from the longitudinal-Varestraint test are summarized in Table 7.

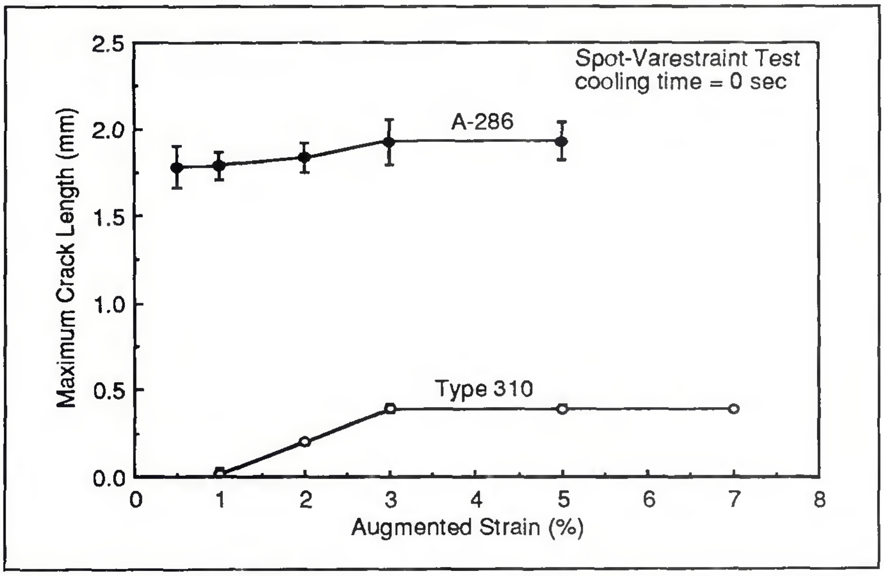

Fig. 14 — On-heating spot-Varestraint test results of A-286 and Type 310 showing the width of the cracked HAZ at different augmented strain levels.

Spot-Varestraint Test Results

The on-heating spot-Varestraint test results for both A-286 and Type 310 alloys are shown in Fig. 14. Because there was no time for the HAZ to cool before cracking occurred, the maximum HAZ crack length (MCL) represented the width of the cracked HAZ under a specific strain level when the HAZ was at peak temperature. For Type 310 stainless steel, above a threshold strain level of 1%, the MCL increased as augmented strain increased up to 3%. Above 3% strain, designated the saturated strain, the MCL was essentially constant at 0.39

mm (0.015 in.) from the fusion boundary.

A threshold strain could not be determined for A-286, since significant cracking was observed at the lowest level of augmented strain (0.5%). MCL increased slightly between 0.5% and 3.0% and was essentially constant above 3.0%. The maximum width of the cracked HAZ for A-286, as defined by the MCL in the saturated strain region, was 1.93 mm (0.076 in.). Note that above a saturated strain level, the width of the cracked HAZ during weld heating is essentially constant. As defined previously, the width of the cracked HAZ at the saturated strain level represents the extent of the CSR during heating.

The on-cooling spot-Varestraint tests were performed with a saturated strain of 5% for both alloys to characterize the extent of the CSR during weld cooling. It is important to point out that at a longer cooling time, cracks may propagate across the fusion boundary into the fusion zone. The portion of crack length inside the fusion zone did not represent the material behavior in the HAZ, thus, was not taken into account in this study. Results from the on-cooling tests in Fig. 15 show the on-cooling portion of the CSR. Again, the MCLs represent the distance of crack tips from the fusion boundary. Both alloys behaved in a similar manner, in that the width of the CSR shrank as cooling time increased. For A-286, it disappeared after a cooling time of 4.13 s, while for Type 310 this region persisted for only 0.41 s.

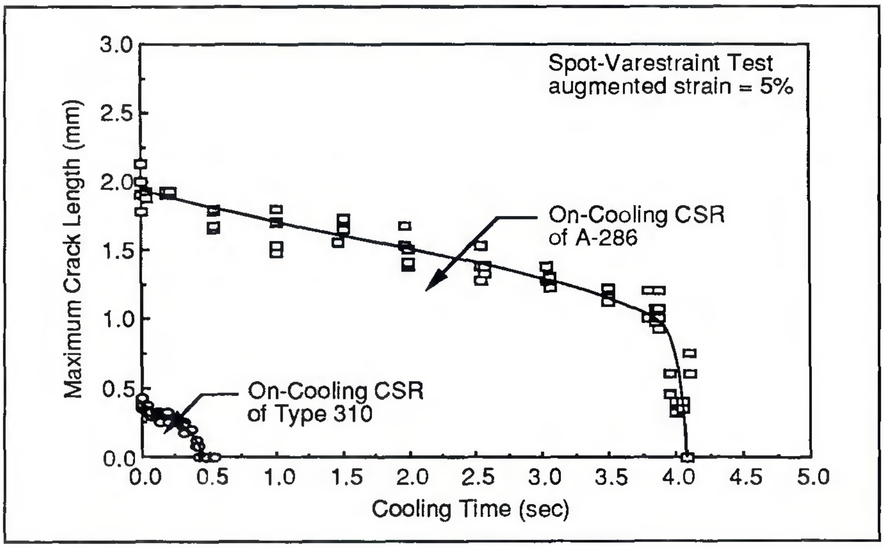

Fig. 15 — On-cooling spot-Varestraint test results of A-286 and Type 310 showing the on-cooling portion of the CSR.

Development of the Thermal CSR Based on the Spot-Varestraint Test Results

The methodologies utilized to develop the thermal CSR based on the spot-Varestraint test results are basically the same as those for the longitudinal-Varestraint test. The on-cooling thermal CSR can be developed by combining the spatial CSR (Fig. 15) and the thermal conditions experienced in the HAZ during testing. The thermal conditions in the HAZ during testing were determined using the implanted thermocouple technique, as described previously. The peak temperatures of thermal cycles at different locations in the HAZ are shown in Fig. 16 with an approximate gradient of 101°C/mm (182°F/0.04 in.) for A-286 and 156°C/mm (281°F/0.04 in.) for Type 310. The peak temperature at the fusion boundary was determined to be 1422°C (2592°F) for A-286 and 1386°C (2527°F) for Type 310. These temperatures are believed to approximate the liquidus temperatures (T_L) since these data are very close to published melting ranges (1370°–1430°C for A-286 and 1400°–1450°C for Type 310) (Ref. 59).

In conjunction with the thermal cycle data in the HAZ, Fig. 15 can be translated to represent the on-cooling portion of the thermal CSR, as schematically shown in Fig. 17. Point A represents the instantaneous liquidus temperature (T_L). Point B represents the crack tip temperature determined with no cooling time (t_c = 0 s). The temperature at Point B (T_B) can be derived following the equation:

$$T_B = T_L - (MCL \times G_T) \qquad (3)$$

where, G_T is the gradient of peak temperatures during spot-Varestraint testing, and MCL is the maximum HAZ crack length performed with no cooling time (t_c = 0). Temperatures along line AB represent different peak temperatures achieved in the HAZ. Since the cooling time is equivalent to the period after weld pool has passed in a continuous weld. Line AA′ would then represent various temperatures at the fusion boundary after arc extinction. Point A′ locates the greatest cooling time in the spot-Varestraint test above which cracks do not propagate across the fusion boundary into the HAZ. The temperature at the fusion boundary (T_{FB}) after arc extinction can be derived from the cooling time (t_c) following the equation:

$$T_{FB} = T_L - (CR_T \times t_c) \qquad (4)$$

where, CR_T is the average cooling rate at the fusion boundary over a period of t_c. Line BA′ represents crack tip temperatures at various cooling times. These crack tip temperatures (T_{tip}) can be derived using a point along line AB with the same distance from the fusion boundary as a reference and following the equation:

$$T_{tip} = T_P - (t_c \times CR_T) \qquad (5)$$

where, T_P = the peak temperature of a HAZ thermal cycle which the point of interest experienced during spot-Varestraint testing; t_c = the cooling time over which cracking is observed at the point of interest; CR_T = the average cooling rate of a thermal cycle with a peak temperature of T_P from the peak temperature over a time period of t_c.

For example, Point E and E′ are in the same thermal cycle with a peak temperature equal to T_E, as they are equidistant from the fusion boundary. Cracking at

Table 8 — Pertinent Thermal CSR Data Obtained from the Spot-Varestraint Test

	A-286	Type 310
MCL (t_c = 0)	1.93 mm	0.39 mm
$t_{c,NST}$	4.10 s	0.20 s
$t_{c,TL}$	4.13 s	0.41 s
G_T	101°C/mm	156°C/mm
CR_T at NST from NST over $t_{c,NST}$, (E-E′ in Fig. 17)	68°C/s	140°C/s
CR_T at T_L from T_L over $t_{c,TL}$, (A-A′ in Fig. 17)	94°C/s	220°C/s

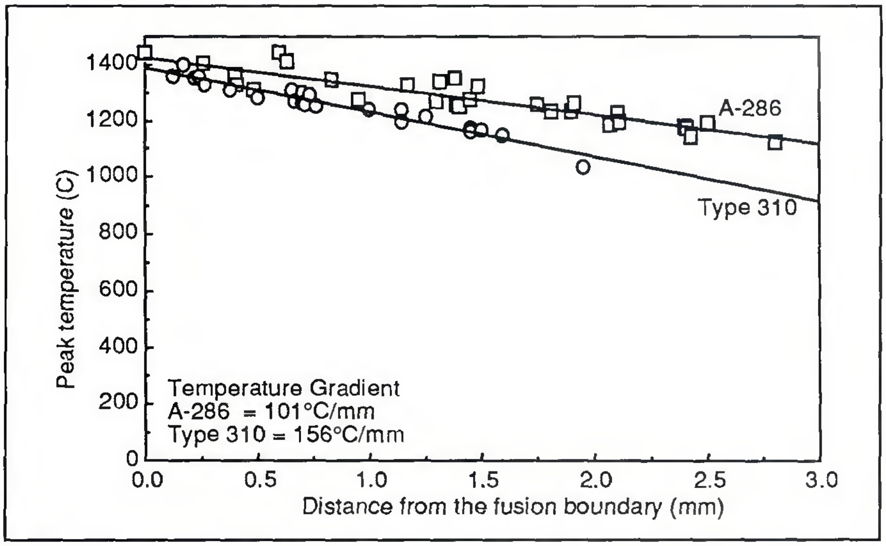

Fig. 16 — Peak temperatures of weld thermal cycles at different locations in the HAZ for A-286 and Type 310 during spot-Varestraint testing.

point E is observed over a cooling time period of $t_{E'}$. Thus, the temperature in the thermal cycle reaches point E' ($T_{E'}$) at a time period $t_{E'}$ after it has achieved the peak. Mathematically, $T_{E'} = T_E - (CR_T \times t_{E'})$, where, CR_T is the average cooling rate from T_E over a period of $t_{E'}$. Pertinent thermal CSR data for alloys A-286 and Type 310 obtained from the spot-Varestraint test are summarized in Table 8.

Discussion

Results from this study have indicated that the HAZ thermal CSR of a material can be determined using any of the three tests. In the hot-ductility test, the HAZ thermal CSR is circumscribed by the NDT isotherm for the on-heating portion, and the various DRTs for the on-cooling portion — Fig. 7. In the longitudinal-Varestraint test, the profile of the crack tip temperatures in the HAZ for the test performed with the saturated strain determines the envelope of the HAZ thermal CSR — Fig. 13. In the spot-Varestraint test, the crack tip temperature of the on-heating tests performed with the saturated strain determines the transition temperature of the on-heating thermal CSR, and the various crack tip temperatures of the on-cooling tests performed with the saturated strain enclose the on-cooling thermal CSR — Fig. 17. The correlation and the methodology of data interpretation of the three tests can be illustrated by characterizing the ductility of the material in the thermal CSR obtained from the longitudinal- and spot-Varestraint tests and comparing the extent of the HAZ thermal CSR obtained from the three methods.

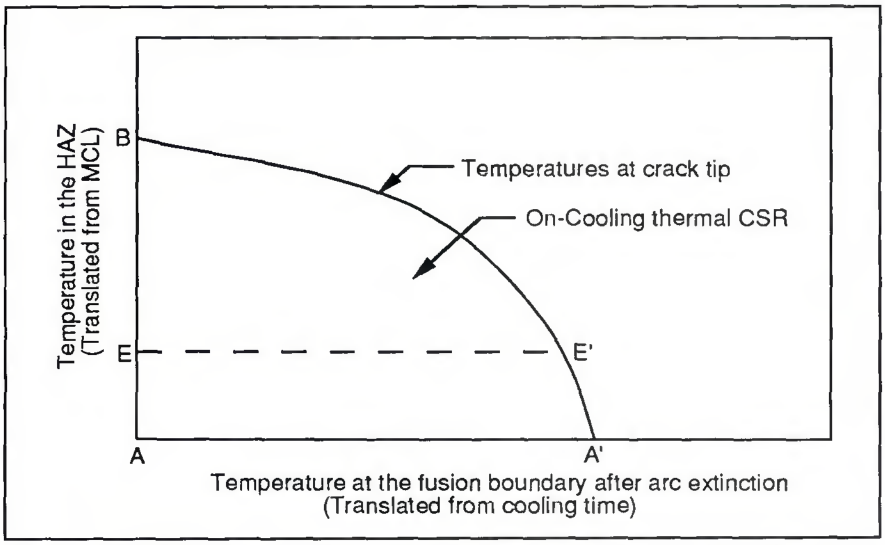

Fig. 17 —Schematic illustration of the on-cooling portion of the thermal CSR obtained from the spot-Varestraint test.

Characterization of the Ductility of Material in the Thermal CSR Obtained from Longitudinal- and Spot-Varestraint Tests

One of the important criteria assumed in the development of liquation theories is that cracking results from the localized loss of ductility. In order to prevent liquation cracks from propagating, the material must exhibit sufficient ductility to accommodate the thermally induced and/or externally applied strain. Based on this criterion, to a first approximation, it would be appropriate to assume that the material at the crack tip exhibits localized ductility with the magnitude equal to the applied augmented strain during both the longitudinal- and spot-Varestraint testing. Thus, in conjunction with the thermal cycle data, Figs. 11 and 14 can be translated to physically show the localized ductility of the material at different temperatures during weld heating as shown in Fig. 18 for the longitudinal-Varestraint test and Fig. 19 for the spot-Varestraint test. In these figures, the localized ductility is analogous to the augmented strain. The temperature of the material represents the temperature at the crack tip (T_{tip}) during testing, which is translated from the MCL following the equation:

$$T_{tip} = T_L - (MCL \times G_T) \qquad (6)$$

Thus, results from the on-heating portion of the longitudinal-Varestraint test (Fig. 18) showed that A-286 exhibited substantial localized ductility (greater than 7% in this case) for temperatures below 1194°C (2181°F). As the temperature increased beyond 1194°C, the localized ductility dropped dramatically to 3%, and further decreased to 0.5% at higher temperatures below T_L. In contrast, results from the on-heating spot-Varestraint tests (Fig. 19) indicated that A-286 exhibited considerable localized ductility (greater than 5% in this case) for temperatures below 1227°C (2241°F). The localized ductility dropped substantially to 3% as the temperature increased beyond 1227°C. With a further increase in temperature, the localized ductility decreased gradually to 0.5% at a temperature of 1240°C, and A-286 exhibited essentially no ductility (less than 0.5%) for the temperature range between 1240°C (2264°F) and T_L. On the other hand, Type 310 (Fig. 19) exhibited greater than 7% localized ductility for temperatures below 1325°C (2417°F). The localized ductility dropped rapidly to 3% as the temperature exceeded 1325°C, and further decreased to approximately 1% at temperatures slightly below T_L.

Note that there is a transition temperature, 1194°C or 1227°C for A-286 as obtained from longitudinal- and spot-Varestraint, respectively, and 1325°C for Type 310, above which the localized ductility of the material dramatically drops to essentially zero. The temperature range between T_L and the transition temperature defines the extent of the on-heating thermal CSR. In order to determine this transition temperature, it is essential the saturated augmented strain be employed during both longitudinal- and spot-Varestraint testing. It is apparent that saturated augmented strain is one of the important parameters for both of these tests, yet the importance of this parameter has generally been neglected by most investigators who have used these two tests to quantify liquation cracking.

It is interesting that the transition temperatures for A-286 defined with the longitudinal-and spot-Varestraint tests are essentially the same, if reasonable experimental error is taken into account. However, the localized ductility in the on-heating thermal CSR is inconsistent. This discrepancy can be rationalized by considering the different local variations in strain accommodation on the specimen surface during testing.

As shown in Fig. 20, the HAZ liquation cracks are parallel to each other in the longitudinal-Varestraint test. Because the applied augmented strain is theoretically calculated based on the elongation of the top surface of the specimen, the opening of the cracks would accommodate some amount of the applied strain. The as-tested specimen surface clearly showed that the opening of the crack is wider at the trailing edge of the weld pool and becomes narrower toward the welding direction. This implies that the strain distribution is not uniform with a greater strain at the trailing edge of the weld pool. Thus, the actual augmented strain for the crack located at the transition between on-heating and on-cooling regions would be lower than the calculated strain. In contrast, the HAZ liquation cracks are radially oriented relative to the weld center in the spot-Varestraint test, as shown in Fig. 21. The crack with a maximum length is always the widest and located perpendicular to the longitudinal dimension of the specimen, indicating that the localized strain was highest at that point. It is postulated, therefore, the localized augmented strain is greater than the calculated strain at this location. Based on this argument, it follows that the difference in the localized strain distribution in the longitudinal- and spot-Varestraint tests results in the difference in the experimentally determined localized ductility in the on-heating thermal CSR from these two tests, with a greater localized ductility in the former.

It was observed that both the longitudinal- and spot-Varestraint test specimens did not conform perfectly to the surface of the die block. Specimens in both tests tended to kink slightly at the highest augmented strain level (7%). The kinking of the specimen may thus result in a higher applied strain than that calculated. However, it did not affect the ductility transition temperature (Figs. 18 and 19), since it was determined at a saturated strain level of 3% for both alloys. As shown in Figs. 18 and 19, even with a higher level of augmented strain (>3%), the transition temperature does not change and, thus, specimen kinking did not influence the results.

The localized ductility in the on-cooling portion of the thermal CSR determined with the longitudinal- and spot-Varestraint was not evaluated in this study. However, it is definitely less than 5% for the two alloys investigated, since 5% augmented strain was employed for the on-cooling spot-Varestraint tests, and the CSR was obtained for A-286 at 5% augmented strain from the longitudinal-Varestraint test. Thus, the thermal CSR shown in Figs. 13 and 17 represents a regime within which the material (both A-286 and Type 310) exhibits less than 5% ductility (or perhaps 3%, since 3% is the saturated strain for both alloys in both tests).

Considering the complexity of the strain field during the longitudinal- and

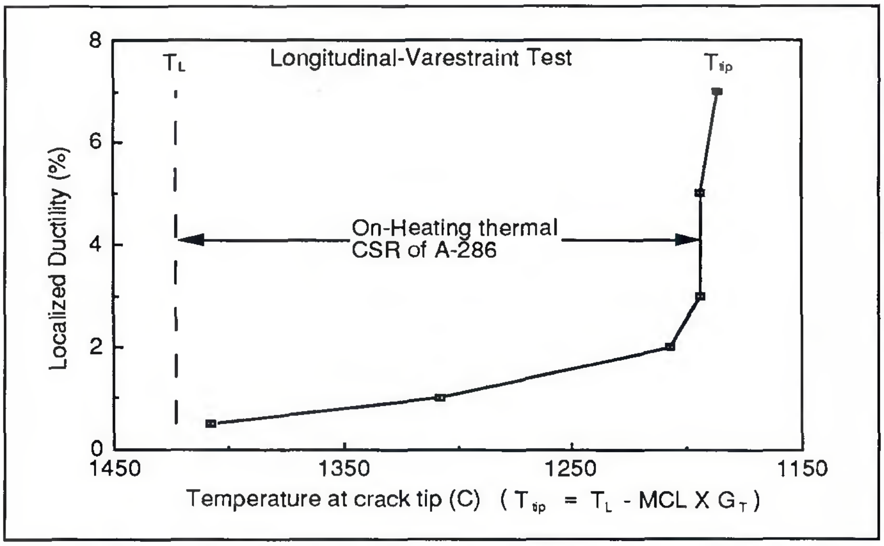

Fig. 18 — The localized ductility in the on-heating thermal CSR of A-286 obtained from the longitudinal-Varestraint test.

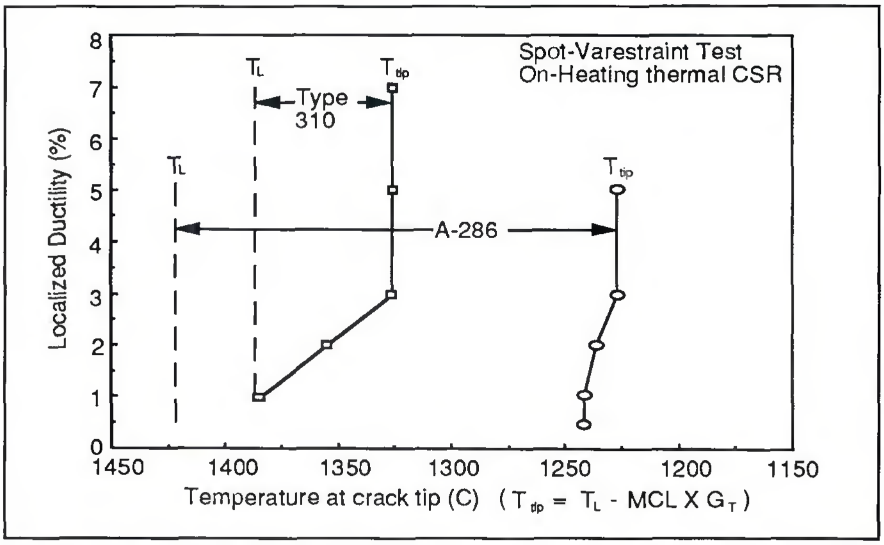

Fig. 19 — The localized ductility in the on-heating thermal CSR of A-286 and Type 310 obtained from the spot-Varestraint test.

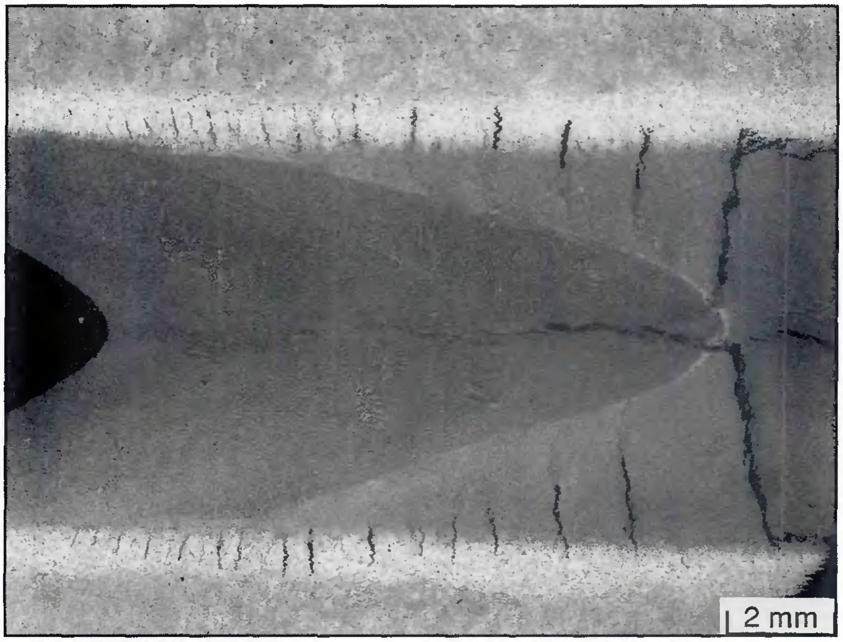

Fig. 20 — A micrograph showing the HAZ liquation cracks of A-286 tested with 5% augmented strain from the longitudinal-Varestraint test. The welding direction is from right to left.

spot-Varestraint testing and different thermal and mechanical conditions for hot-ductility testing, it would be appropriate to equate this very low-ductility thermal CSR to the nil-ductility region (NDR) as determined from the hot-ductility test. The equivalence between the CSR and the NDR provides experimental evidence for the criterion assumed in the development of liquation cracking theories, which states that liquation cracking results from the localized loss of ductility.

Correlation and Interpretation of Test Results Obtained from the Three Methods

Two basic elements with metallurgical significance can be visualized in the development of the thermal CSR. These are the extent of the thermal CSR during weld heating and the BTR on cooling. The correlation between the theoretical hypothesis and the experimental results can be demonstrated by comparing the magnitude of these two elements. As listed in Table 9, very good correlation was obtained for A-286 and Type 310 stainless steels among the three tests.

The development of this correlation also clarifies the interpretation of results from the three tests. Physically, the temperature range between the T_L and NDT represents the extent of the thermal CSR during weld heating. This temperature range correlates with the temperature range over which the MCL occurs at the transition between on-heating and on-cooling regions in the longitudinal-Varestraint test performed with saturated strain. It also correlates with the temperature range over which the MCL occurs in the spot-Varestraint test performed with saturated strain at no cooling time ($t_c = 0$). The temperature range between a peak temperature and the corresponding DRT is the temperature range in a cooling cycle within which the material exhibits negligible ductility, previously defined as the BTR. This temperature range in turn correlates with the cooling time (t_c) over which cracking is observed in the spot-Varestraint test, and the on-cooling portion of the cracked HAZ length (CHL_{OC}) in the longitudinal-Varestraint test. Despite the difference in testing techniques, the correlation obtained for both A-286 and Type 310 is excellent, reinforcing the complementary nature of these techniques for predicting HAZ liquation cracking. This good correlation also provides evidence that the thermal CSR is a material-specific parameter, and a true quantification of HAZ liquation cracking susceptibility.

Application to Actual Welding Conditions

Although the thermal CSR is developed using weldability testing techniques, it is a material-specific parameter and can be applied to any of the conventional fusion welding processes. The application of the thermal CSR in a continuous weld can be clearly demonstrated with the longitudinal-Varestraint test as illustrated in Figs. 10 and 20. Table 10 summarizes the procedures for determining the thermal CSR using the hot-ductility, longitudinal- and spot-Varestraint tests. It is of importance to note that the shape and size of the thermal CSR reflects the compositional and metallurgical nature of the material and is independent of any process or restraint factors. The thermal CSR allows comparison of cracking susceptibility among different materials. Using this methodology, the thermal CSR surrounding a moving weld pool has been determined for A-286 and Type 310, as shown in Fig. 22. It is clear that A-286 exhibits a larger BTR and correspondingly wider thermal CSR than Type 310, indicating that A-286 would exhibit greater extent of HAZ liquation cracking than Type 310 under the same thermal and restraint conditions.

In applying this material-specific envelope to actual welding conditions, the spatial extent of the CSR traveling with the weld pool can be determined as a function of the welding parameters, which determine the thermal conditions in the HAZ. Table 11 provides a transformation matrix for determining the magnitude of the thermal and spatial CSR. As a result, the thermal envelope determined via hot-ductility, spot- and longitudinal-Varestraint weldability tests can be directly applied to actual welding situations if the thermal gradient (G_W) and cooling rate (CR_W) can be measured or derived empirically. The contribution of the welding process/parameter factor in cracking susceptibility can also be visualized from the construction of the spatial CSR.

Evaluation of Traditional Methodologies

The development of this methodology has provided a means to link together weldability test results, cracking theories and material properties, and to elucidate the interpretation of the hot-ductility, spot- and longitudinal-Varestraint test results. The utility of traditional methodologies can also be evaluated based on this approach as discussed below.

Hot-Ductility Test

The construction of the NDR using the hot-ductility test was first demonstrated by Duvall, *et al.* (Refs. 32, 33). Unfortunately, they could not develop a relationship between the NDR and HAZ liquation cracking susceptibility. Based on a rough calculation of the weld size, he suggested that HAZ liquation cracks propagated outside of the NDR (*i.e.*, via solid-state cracking) and the amount and rate of ductility recovery were the most significant factors governing liquation cracking susceptibility. Despite the high levels of strain used in this investigation during spot- and longitudinal-Varestraint testing, cracks were never observed to propagate outside of the NDR. Thus, the importance of ductility recovery below the DRT, as suggested by Duvall, *et al.*, appears to be negligible based on the results from both A-286 and Type 310 stainless steels.

The NST-DRT temperature range has been utilized extensively as a quantitative cracking index (Refs. 11, 27, 30, 31). This index is restrictive in that it only represents the BTR at a specific location in the HAZ. Since the highest peak temperature that can be easily achieved in the hot-ductility test is in the vicinity of the NST, this approach only provides information for a point in the HAZ that is removed from the fusion boundary. When considering that HAZ liquation cracking is commonly observed in the region immediately adjacent to the fusion boundary, this cracking index may not be representative of actual behavior or predictive of liquation cracking susceptibility. This is particularly true if the difference between T_L and the NST is large. This problem is further exacerbated when peak temperatures below the NST are used to develop on-cooling hot ductility behavior, as is the case in many of the published reports which use hot-ductility data to predict HAZ liquation cracking susceptibility.

The hot strength criterion proposed in 1960s (Refs. 27–29) is commonly utilized to rationalize the inconsistency between the hot-ductility results and cracking observed in the field experience. However, considering the fact that all materials exhibit extremely low strength in the temperature range in which cracking occurs, the elastic strain induced by this hot strength would be negligible. In addition, most alloys exhibit a critical level of threshold strain for cracking in the spot- and longitudinal-Varestraint testing (*e.g.*, 1% for Type 310 in Fig. 14). The observation of significant threshold strain to cause cracking indicates that the materials have the ability to resist cracking even under a substantial applied stress. This suggests, therefore, that it is the hot ductility rather than hot strength that dominates liquation cracking.

Spot-Varestraint Test

The conventional cracking indexes for the spot-Varestraint test, the threshold strain to cause cracking or the degree of cracking (MCL or TCL) over arbitrary augmented strain levels and an arbitrary cooling time, are even more complicated from a metallurgical stand-

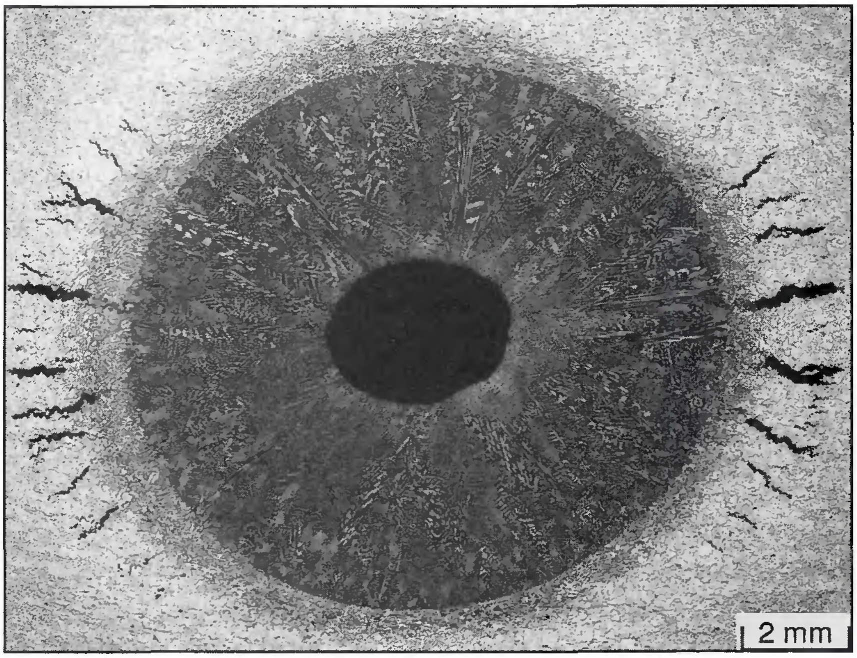

Fig. 21 — A micrograph showing the HAZ liquation cracks of A-286 tested with 5% augmented strain from the spot-Varestraint test.

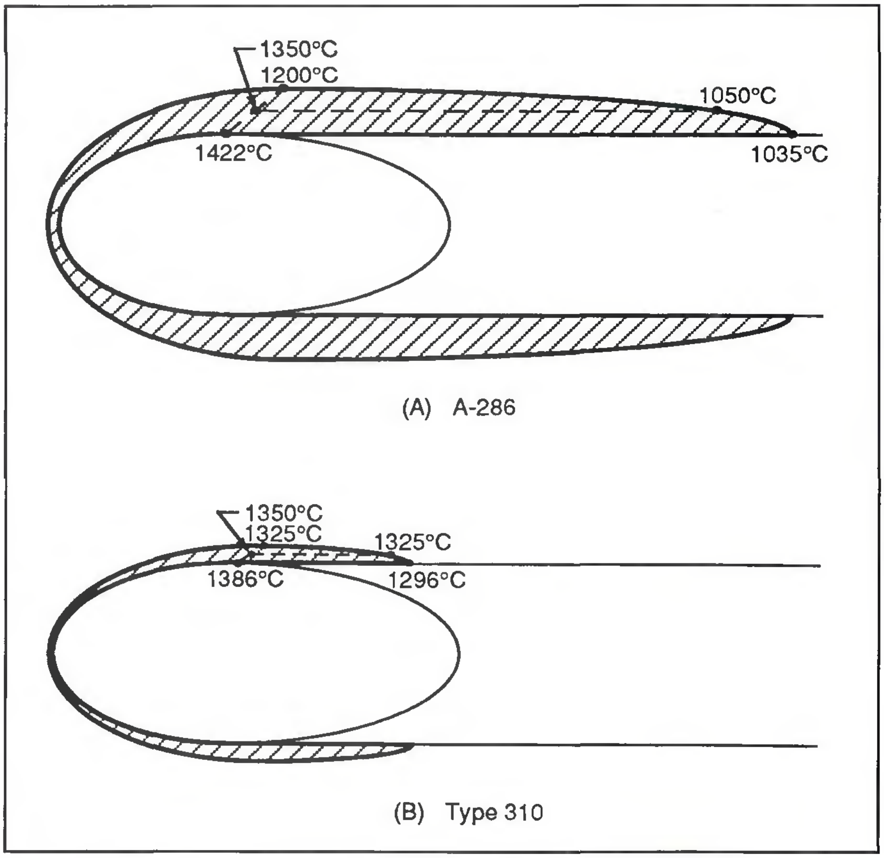

Fig. 22 — Thermal CSR of A-286 and Type 310 stainless steels.

Table 9 — Correlations among the Hot-Ductility, Spot- and Longitudinal-Varestraint Test Results

	Hot-Ductility Test	Spot-Varestraint Test	Longitudinal-Varestraint Test
A-286, Extent of the on-heating CSR	$T_L - NDT =$ 1422 − 1200 = 222°C	$MCL \times G_T =$ 1.93 × 101 = 195°C	$MCL \times G_T =$ 0.80 × 286 = 229°C
Type 310, Extent of the on-heating CSR	$T_L - NDT =$ 1386 − 1325 = 61°C	$MCL \times G_T =$ 0.39 × 156 = 60°C	Not Determined
A-286, BTR at NST	$NST - DRT_{NST} =$ 1350 − 1050 = 300°C	$t_c \times CR_T =$ 4.10 × 68 = 279°C	$CR_T \times CHL_{OC}/V_T =$ 66 × 11.5/2.54 = 299°C
Type 310, BTR at NST	$NST - DRT_{NST} =$ 1350 − 1325 = 25°C	$t_c \times CR_T =$ 0.20 × 140 = 28°C	Not Determined

point. First, the crack length (either MCL or TCL) does not provide a material-specific quantification; rather, it represents a specific material/process/restraint combination. Any variation in the test conditions such as the welding parameters and the augmented strain level would affect the test results. Second, the saturated strain has been found to be the parameter which must be used to uniquely determine the size of the CSR. As shown in Fig. 14, the MCL is dependent on the augmented strain for the strain level below the saturated strain. Thus, the MCL determined below the saturated strain, such as in most of the published literature, would only represent part of the CSR. It does not provide a comprehensive measure of cracking susceptibility. It is also of importance to note that the MCL determined in this manner is very sensitive to the localized strain distribution of samples during testing. Thus, test results from a laboratory may not be easily reproduced in another laboratory due to the difference in equipment setup. Third, the cooling time has been proved to be the parameter which governs the HAZ temperature during testing and, thus, the on-cooling behavior of material. Tests performed with an arbitrary, fixed cooling time will only reveal a specific width of the on-cooling CSR as shown in Fig. 15. The use of unsaturated strain level during testing would, then, only reveal part of this specific width and increase the complexity of the test results in relation to the metallurgical aspects of liquation cracking susceptibility. This specific width of the CSR would neither correlate with the on-cooling behavior obtained from the hot-ductility test nor reflect the cracking behavior of the material during actual welding.

The metallurgical significance of the MCL can also be revealed from this study. By representing MCL as the distance from the fusion boundary to the crack tip, it can be directly correlated with the extent of the CSR. Notice that this manner of representation of the MCL also dramatically reduces the human error in crack length measurement. Historically, this cracking index has not been used as extensively as the TCL in the published literature. In the spot-Varestraint test, the TCL represents the cumulative length of all cracks with the same thermal conditions at different strain levels. It is not material-specific and may be influenced by grain size and strain localization at the grain boundary. As a result, TCL is not metallurgically significant with respect to HAZ liquation cracking.

Since spot-Varestraint was modified from the original Varestraint test, the terminologies utilized in quantifying the degree of cracking (MCL or TCL) were also adopted. Physically, the MCL in all three types of Varestraint tests (spot, longitudinal and transverse) characterizes a region over which cracking occurs. However, the thermal histories in this cracked region along the crack are different among these tests. In the Transvarestraint test, the weld centerline crack falls in the same thermal cycle (Ref. 10). In the case of HAZ cracks in the longitudinal- and spot-Varestraint tests, the crack which is perpendicular to the longitudinal direction of the sample follows different thermal cycles in the HAZ, but cracking occurs at the same instant relative to the peak temperature. In the case of solidification cracks in the longitudinal-Varestraint test, cracking occurs following different thermal cycles and at different instants relative to the peak temperature. As a result of the difference in thermal history of the cracks generated in the three tests, the cracking temperature range in the Transvarestraint test determined by the MCL defines the BTR. The HAZ cracking temperature range determined by the MCL in both the longitudinal- and spot-Varestraint tests, on the other hand, defines a thermal width of the cracked region.

Table 10 — Development of the Thermal CSR (Fig. 7)

Point/ Line	Theoretical Quantity	Hot Ductility Test	Spot-Varestraint Test	Longitudinal-Varestraint Test
A	T_L	—	T_P at fusion boundary	T_P at fusion boundary
CB	NDT	NDT	$T_L - (MCL \times G_T)$	$T_L - (MCL \times G_T)$
E	NST	NST	—	—
E′	DRT_{NST}	DRT_{NST}	$NST - (t_{c,NST} \times CR_T)$	$T_L - CR_T \times CHL_{OC,NST}/V_T$
BE′	DRT's	DRT's	T_{tip} as function of t_c	T_{tip} as function of CHL_{OC}
E′A′	DRT's	—	T_{tip} as function of t_c	T_{tip} as function of CHL_{OC}
A′	DRT_{TL}	—	$T_L - (t_{c,TL} \times CR_T)$	$T_L - CR_T \times CHL_{OC,TL}/V_T$

Longitudinal-Varestraint Test

The discussion of the conventional cracking indexes for the longitudinal-Varestraint test, TCL or MCL, follows that for the spot-Varestraint test, except that TCL is the cumulative length of all cracks with the same strain level at different thermal conditions in the longitudinal-Varestraint test. Both the MCL and TCL cracking indexes represent results for a specific material/process/ restraint combination. The magnitude of these indexes would vary if different welding parameters or augmented strain are employed. The CHL criterion, proposed by Lundin, *et al.* (Ref. 14), can be normalized with the thermal conditions experienced during testing to obtain a BTR, if the tests are performed with a saturated strain and only the on-cooling portion of the CHL (CHL_{OC}) is considered, as illustrated in Fig. 10 and Table 11. However, it is very unlikely that the CHL_{OC} at a specific location in the HAZ can be precisely determined without the development of the entire CSR.

Summary

This paper has described an experimental approach that allows HAZ liquation cracking susceptibility to be quantified in a manner that is metallurgically significant and material-specific. Methodologies have been developed and tested for defining the thermal crack-susceptible region (CSR) for a material. Any one of three weldability tests can be used to quantify the thermal CSR, namely, the Gleeble hot-ductility test, and the spot- and longitudinal-Varestraint tests. The results presented here have also provided new insight into the interpretation and correlation of test data for each of these tests and form the basis of a unified approach for defining a material-specific temperature regime within which HAZ liquation cracking occurs. Recent results have shown that this methodology can also be successfully applied to other materials, including Alloy 625 and aluminum Alloy 6061 (Refs. 60, 61).

During the development of this methodology some inherent limitations in utilizing any of the three tests for predicting the occurrence of HAZ liquation cracking were also identified. Although the thermal CSR represents the temperature regime over which HAZ liquation cracking may occur, it only serves as an indirect measure of the actual cracking susceptibility. In order to fully quantify this susceptibility during welding, other factors such as ductility within the BTR, the effect of liquid healing and local HAZ strain accommodation must be considered. Unfortunately, it is very difficult to incorporate these factors when interpreting weldability test data. As a consequence, the methodology developed here, while providing a material-specific quantification of HAZ liquation cracking, cannot easily accommodate the variations in weld restraint that often dictate the occurrence and severity of cracking.

Despite these limitations, the development of this methodology has shown that the Gleeble hot-ductility and Varestraint tests are effective tools for both quantifying the HAZ liquation cracking susceptibility in terms of the size of the thermal CSR and developing a fundamental understanding of the liquation phenomena. Part 2 of this investigation will describe the metallurgical behavior in the CSR in support of this test methodology.

Table 11 — Transformation Matrix for the Derivation of the Thermal and Spatial CSR

	Test Result	Thermal CSR	Spatial CSR
A. The Hot-Ductility Test			
Width of CSR	$T_L - NDT$	$T_L - NDT$	$(T_L - NDT)/G_W$
BTR	$T_P - DRT$	$T_P - DRT$	$(T_P - DRT) \times V_W/CR_W$
B. The Longitudinal-Varestraint Test			
Width of CSR	MCL	$MCL \times G_T$	$MCL \times G_T/G_W$
BTR	CHL_{OC}	$CHL_{OC} \times CR_T/V_T$	$CHL_{OC} \times CR_T/V_T \times V_W/CR_W$
C. The Spot-Varestraint Test			
Width of CSR	MCL	$MCL \times G_T$	$MCL \times G_T/G_W$
BTR	t_c	$t_c \times CR_T$	$t_c \times CR_T \times V_W/CR_W$

Conclusions

1) A new methodology has been developed for quantifying HAZ liquation cracking susceptibility. This methodology quantifies a thermal crack-susceptible region in the HAZ in which HAZ liquation cracking may occur. It is a material-specific parameter and represents a true quantification of HAZ liquation cracking susceptibility. This region can be determined using the Gleeble hot-ductility, spot- or longitudinal-Varestraint tests.

2) The thermal crack-susceptible region can be described by two basic elements: the extent of the crack-susceptible region during weld heating and the brittle temperature range on cooling. The temperature range between the liquidus (T_L) and nil-ductility temperature (NDT) in the hot-ductility test represents the extent of the on-heating thermal crack-susceptible region. This temperature range correlates with the temperature range over which the maximum crack length occurs at the transition between on-heating and on-cooling regions in the longitudinal-Varestraint test performed with saturated strain. It also correlates with the temperature range over which the maximum crack length occurs in the spot-Varestraint test performed with saturated strain for no cooling time after arc extinction.

3) The temperature range between the peak temperature (T_P) and the corresponding ductility recovery temperature (DRT), as obtained from the hot-ductility test, represents the brittle temperature range (BTR). This temperature range in turn correlates with the cooling time over which cracking is observed in the spot-Varestraint test, and the on-cooling portion of the cracked HAZ length in the longitudinal-Varestraint test.

4) The localized ductility within the thermal crack-susceptible region is essentially zero. These results provide experimental evidence supporting the criterion assumed in the development of liquation cracking theories, which states that liquation cracking results from the localized loss of material ductility.

5) The importance of saturated augmented strain in both the longitudinal- and spot-Varestraint tests was evaluated. The saturated strain refers to the applied strain above which the maximum crack length remains constant. It was found that saturated strain conditions must be used to uniquely define the temperature above which the ductility of the material drops to essentially zero. This temperature correlates to the on-heating nil-ductility temperature in the hot-ductility test.

6) The importance of the cooling time in the spot-Varestraint test was evaluated. Cooling time is defined as the time period between arc extinction and specimen bending and is the parameter which governs the temperature in the HAZ during on-cooling spot-Varestraint testing. By varying the cooling time, the on-cooling crack-susceptible region can be determined.

7) For the A-286 stainless steel tested in this study, the extent of the on-heating thermal crack-susceptible region is 222°C. The brittle temperature range at the location of the nil-strength temperature is 300°C. The brittle temperature range at the fusion boundary is 387°C.

8) For the Type 310 stainless steel tested in this study, the extent of the on-heating thermal crack-susceptible region is 61°C. The brittle temperature range at the location of the nil-strength temperature is 25°C. The brittle temperature range at the fusion boundary is 90°C.

Acknowledgments

The authors would like to acknowledge the members of Edison Welding Institute for providing financial support for this work. The generosity of Rolled Alloys, for providing the Type 310 stainless steel, is also appreciated.

References

1. Hemsworth, B., Bonizewski, T., and Eaton, N. F. 1969. Classification and definition of high-temperature welding cracks in alloys. *Metal Construction and British Welding Journal* 1(2):5–16.

2. Lippold, J. C., Harwig, D. E., Ernst, S. C., and Nelson, T. 1989. Development of a weldability test data base WELDTEST. unpublished research. Edison Welding Institute. Columbus, Ohio.

3. Baeslack, W. A. III, and Lippold, J. C. 1987. Evaluation of weldability testing techniques. *Proceedings of EWI Annual North American Welding Research Seminar on The Influence of New Materials Developments on Weldability*. Columbus, Ohio.

4. Lippold, J. C. 1988. Physical simulation of welding: a perspective on weldability testing. *Proceedings of International Symposium on Physical Simulation of Welding, Hot*

Forming and Continuous Casting Processes. Ottawa, Canada.

5. Prokhorov, N. N. 1962. The technological strength of metals while crystallizing during welding. *Welding Production* 9(4):1–8.

6. Prokhorov, N. N., and Prokhorov, N. Nikol. 1971. Fundamentals of the theory for technological strength of metals while crystallizing during welding. *Trans. JWS* 2(2):109–117.

7. Savage, W. F., and Lundin, C. D. 1965. The Varestraint test. *Welding Journal* 34(10):433-s to 442-s.

8. Lundin, C. D., Lingenfelter, A. C., Grotke, G. E., Lessmann, G. G., and Mathews, S. J. 1982. The Varestraint test. Welding Research Council Bulletin No. 280.

9. Savage, W. F., Nippes, E. F., and Goodwin, G. M.. 1977. Effect of minor elements on hot cracking tendencies of Inconel 600. *Welding Journal* 56(8):245-s to 253-s.

10. Senda, T., Matsuda, F., Takano, G., Watanabe, K., Kobayashi, T., and Matsuzaka, T. 1971. Fundamental investigations on solidification crack susceptibility for weld metals with Transvarestraint test. *Trans. JWS* 2(2):1-22.

11. Donati, J. R., and Zacharie, G. 1974. Evaluation of tendency toward hot crack in the welding heat-affected zone of austenitic 18-10 stainless steels. *Revue de Metallurgie* 71(12):905-915.

12. Ogawa, T., and Tsunetomi, E. 1982. Hot cracking susceptibility of austenitic stainless steels. *Welding Journal* 61(3):82-s to 93-s.

13. Lundin, C. D., Lee, C. H., and Menon, R. 1988. Hot ductility and weldability of free machining austenitic stainless steel. *Welding Journal* 67(10):119-s to 130-s.

14. Lundin, C. D., and Qiao, C. Y. P. 1991. Weldability of nuclear grade stainless steels. *Proceedings of the International Conference on New Advances in Welding and Allies Processes.* Beijing, China.

15. Katoh, M., and Kerr, H. W. 1987. Investigation of heat-affected zone cracking of GTA welds of Al-Mg-Si alloys using the Varestraint test. *Welding Journal* 66(12):360-s to 368-s.

16. West, S. L., Baeslack, W. A. III, and Kelly, T. J. 1989. Morphology of weld heated-affected zone liquation cracking in Ta-modified cast alloy 718. *Metallography* 23(3):219-229.

17. Thompson, R. G., Cassimus, J. J., Mayo, D. E., and Dobbs, J. R. 1985. The relationship between grain size and microfissuring in alloy 718. *Welding Journal* 64(4):91-s to 96-s.

18. Thompson, R. G. 1988. Microfissuring of alloy 718 in the weld heat-affected zone. *Journal of Metals* 40(7):44-48.

19. Lippold, J.C., Baeslack, W. A. III, and Varol, I. 1992. Heat-affected zone liquation cracking in austenitic and duplex stainless steels. *Welding Journal* 71(1):1-s to 14-s.

20. Kujanpää, V. P., David, S. A., and White, C. L. 1987. Characterization of heat-affected zone cracking in austenitic stainless steel welds. *Welding Journal* 66(8):221-s to 228-s.

21. Lippold, J. C. 1983. An investigation of heat-affected zone hot cracking in alloy 800. *Welding Journal* 62(1):1-s to 11-s.

22. Ernst, S. C., Baeslack, W. A. III, and Lippold, J. C. 1989. Weldability of a high-strength, low-expansion superalloy. *Welding Journal* 68(10):418-s to 430-s.

23. Brooks, J. A. 1974. Effect of alloy modifications on HAZ cracking of A-286 stainless steel. *Welding Journal* 53(11):517-s to 523-s.

24. Lin, W. 1991. A methodology for quantifying heat-affected zone liquation cracking susceptibility. Ph.D. dissertation. The Ohio State University. Columbus, Ohio.

25. Nippes, E. F., Savage, W. F., Bastin, B. T., Mason, H. F., and Curran, R. M. 1955. An investigation of the hot ductility of high-temperature alloys. *Welding Journal* 34(4):183-s to 196-s.

26. Nippes, E. F., Savage, W. F., and Grotke, G. 1957. Further studies of the hot ductility of high-temperature alloys. Welding Research Council Bulletin No. 33.

27. Williams, C. S. 1963. Steel strength and ductility response to arc welding thermal cycles. *Welding Journal* 42(1):1-s to 8-s.

28. Kreischer, C. H. 1963. A critical analysis of the weld heat-affected zone hot ductility test. *Welding Journal* 42(2):49-s to 59-s.

29. Weiss, B., Grotke, G. E., and Stickler, R. 1970. Physical metallurgy of hot ductility testing. *Welding Journal* 49(10):471-s to 487-s.

30. Dahl, W., Duren, C., and Muesch, H. 1973. Susceptibility of austenitic welded joints to hot cracking. IIW Doc. II-660-73.

31. Muesch, H. 1984. Welding of material TP 347 mod. Mannesmann Research Institute. Duisburg, Germany.

32. Owczarski, W. A., Duvall, D. S., and Sullivan, C. P. 1966. A model for heat-affected zone cracking in nickel base superalloys. *Welding Journal* 45(4):145-s to 155-s.

33. Duvall, D. S., and Owczarski, W. A. 1967. Further heat-affected zone studies in heat resistant nickel alloys. *Welding Journal* 46(9):423-s to 432-s.

34. Yeniscavich, W. 1966. A correlation of Ni-Cr-Fe alloy weld metal fissuring with hot ductility behavior. *Welding Journal* 45(8):334-s to 356-s.

35. Yeniscavich, W. 1969. Correlation of hot ductility curves with cracking during welding. *Proceedings of the Symposium on Methods of High-Alloy Weldability Evaluation.* 2-12. Welding Research Council. Troy, N. Y.

36. Arata, Y., Terai, K., Nagai, H., Shimizu, S., and Aota, T. 1977. Fundamental studies on electron beam welding of heat-resistant superalloys for nuclear plants - Report II. *Trans JWRI* 6(1):69–79.

37. Lin, W., Baeslack, W. A., III and Lippold, J. C. 1989. Hot ductility testing of high strength low expansion superalloys. Recent trends in welding science and technology TWR '89. 609–614, ASM International, Materials Park, Ohio.

38. Blum, B. S., and Witt, R. H. 1963. Heat-affected zone cracking in A-286 weldments. *Welding Journal* 42(8):365-s to 370-s.

39. Brooks, J. A., and Krenzer, R. W. 1974. Progress toward a more weldable A-286. *Welding Journal* 53(6):242-s to 245-s.

40. Vagi, J. J., and Martin, D. C. 1956. Welding of high-strength stainless steels for elevated-temperature use. *Welding Journal* 35(3):137-s to 144-s.

41. Brooks, J. A. 1974. Effect of alloy modifications on HAZ cracking of A-286 stainless steel. *Welding Journal* 53(11):517-s to 523-s.

42. Morishige, N., Kuribayashi, M., and Okabayashi, H. 1979. Effects of chemical compositions of base metal on susceptibility to hot cracking in austenitic stainless steel welds. IIW Doc. IX-1114-79.

43. Gooch, T. G., and Honeycombe, J. 1980. Welding variables and microfissuring in austenitic stainless steel weld metal. *Welding Journal* 59(8): 233-s to 241-s.

44. Lundin, C. D., Chou, C. P. D., and Sullivan, C. J. 1980. Hot cracking resistance of austenitic stainless weld metal. *Welding Journal* 59(8):226-s to 232-s.

45. King, B. L. 1966. Weld metal and heat-affected zone cracking in wrought austenitic stainless steels. BWRA Report, C139/A/2/65. The Welding Institute. Cambridge, England.

46. Tamura, H., and Watanabe, T. 1973. Mechanism of liquation cracking in the weld heat-affected zone of austenitic stainless steels. *Trans JWS* 4(1):30–42.

47. Labtech Notebook software package. 1990. Laboratory Technologies Corp., Wilmington, Mass.

48. Demyantsevich, V. P. 1967. Mechanism of hot cracking during welding. *Welding Production* 14(3):1–6.

49. Medovar, B. I. 1954. On the nature of weld hot cracking. Avtom. Svarka 7(4):12–28. *Brutcher Translations No. 3400.*

50. Torpov, V. A. 1957. On the mechanism of hot cracking. Metallovedenie Obrabotka Metallov (6):54–58. *Brutcher Translations No. 3982.*

51. Pumphrey, W. J., and Jennings, P. H. 1948. A consideration of the nature of brittleness above the solidus in castings and welds on aluminum alloys. *Journal of the Institute of Metals* 75:235–256.

52. Pellini, W. S. 1952. Strain theory of hot tearing. *The Foundry* 80(11):125–133.

53. Apblett, W. R., and Pellini, W. S. 1954. Factors which influence weld hot cracking. *Welding Journal* 33(2):83-s to 90-s.

54. Bishop, H. F., Ackerlind, C. E., and Pellini, W. S. 1952. Metallurgy and mechanics of hot tearing. *Trans. American Foundrymans Society* 60:818–833.

55. Borland, J. C., and Younger, R. N. 1960. Some aspects of cracking in welded Cr-Ni austenitic steels. *British Welding Journal* 6(1):9–46.

56. Borland, J. C. 1961. Generalized theory of super-solidus cracking in weld and casting. *British Welding Journal* 7(8):508–512.

57. Borland, J. C. 1979. Fundamentals of solidification cracking in welds. *Welding and Metal Fabrication Part I,* (1/2):19-29. Part II, (3):99–107.

58. Matsuda, F., Nakagawa, H., and Sorada, K. 1982. Dynamic observation of solidification and solidification cracking during welding with optical microscope. *Trans. JWRI* 11(2):67–77.

59. *ASM Metal Handbook.* Properties and selection: stainless steels, tool materials and special-purpose metals. 9th Edition, Vol. 3, ASM International, Materials Park, Ohio.

60. Lin, W., Nelson, T. W., Lippold, J. C., and Baeslack, W. A. III. 1992. A study of the HAZ crack-susceptible region in alloy 625. to be published in *Proceedings of the 3rd International Conference on Trends in Weld-*

ing Research, Gatlinburg, Tenn.

61. Nelson, T. W., Lin, W., and Lippold, J. C. 1992. A study of the HAZ crack-susceptible region in 6061 aluminum alloy. unpublished research. Edison Welding Institute. Columbus, Ohio.

Appendix A

Symbols and Abbreviations

BTR	Brittle temperature range
CHL	Cracked heat-affected zone length
CHL_{OC}	On-cooling portion of the cracked HAZ Length
$CHL_{OC,NST}$	CHL_{OC} at a point in the HAZ which experiences a peak temperature of NST
$CHL_{OC,TL}$	CHL_{OC} at the fusion boundary
CHL_{OH}	On-heating portion of the cracked HAZ Length
CR_T	Average Cooling Rate during weldability testing
CR_W	Average cooling rate for actual welding conditions
CSR	Crack-susceptible region
DRT	Ductility recovery temperature
DRT_{NST}	DRT corresponding to a peak temperature equal to the NST
DRT_{TL}	DRT corresponding to a peak temperature equal to the T_L
FB	Fusion Boundary
G_T	Temperature gradient during weldability testing
G_W	Temperature gradient for actual welding conditions
HAZ	Heat-affected zone
MCL	Maximum crack length
NDR	Nil-ductility region
NDT	Nil-ductility temperature
NST	Nil-strength temperature
PMZ	Partially-melted zone
t_c	Cooling time over which cracking occurs in the spot-Varestraint testing
$t_{c,NST}$	t_c at a point in the HAZ which experiences a peak temperature of NST
$t_{c,TL}$	t_c at the fusion boundary
TCL	Total crack length
T_{FB}	Temperature at the fusion boundary after arc extinction
T_L	Liquidus temperature
T_P	Peak temperature of a thermal cycle
T_{tip}	Temperature at the crack tip during weldability testing
V_T	Travel speed during longitudinal-Varestraint testing
V_W	Travel speed for actual welding conditions

Appendix B

Definition of Terms

Brittle Temperature Range (BTR): The temperature range during weld cooling within which the material is susceptible to liquation cracking due to the localized loss of grain boundary ductility.

Cooling Time (t_C) or Delay Time: The time period between arc extinction and specimen bending for the spot-Varestraint test.

Cracked HAZ Length (CHL): The length of the region in the HAZ, measured parallel to the fusion boundary, over which cracking is observed in the longitudinal-Varestraint test.

Crack-susceptible Region (CSR): The HAZ region, surrounding the weld pool, within which the material is susceptible to liquation cracking due to the localized loss of ductility.

Ductility Recovery Temperature (DRT): Temperature on-cooling from a peak temperature above the NDT at which perceptible ductility (>5%) of the material is apparent.

Maximum Crack Length (MCL): The maximum length of cracks on the as-tested specimen surface in longitudinal- or spot-Varestraint tests. Traditionally, this crack length is measured from tip to tip of a crack. In this study, the MCL represents the distance between the isotherm at the crack tip and the isotherm at the fusion boundary.

Nil-Ductility Region (NDR): A region in the HAZ, surrounding the weld pool, within which the ductility of the material, as determined with the hot-ductility test, is essentially zero.

Nil-Ductility Temperature (NDT): Temperature on-heating at which the ductility of the material drops to zero.

Nil-Strength Temperature (NST): Temperature on-heating at which the strength of the material drops to essentially zero.

Saturated Strain: The applied augmented strain level above which the maximum crack length remains constant, or saturates, for the spot- and longitudinal-Varestraint tests.

Threshold Strain: The applied augmented strain above which cracking occurs in the longitudinal- or spot-Varestraint tests.

Total Crack Length (TCL): Cumulative length of all cracks on an as-tested specimen surface in spot- or longitudinal-Varestraint tests.